Computational modeling enables individual assessment of postprandial glucose and insulin responses after bariatric surgery

Onur Poyraz[1*] **Sini Heinonen**[2,3*] **S. T. John**[1] **Tuure Saarinen**[4] **Anne Juuti**[4]
Pekka Marttinen[1†] **Kirsi H. Pietiläinen**[2,5†]
[1]Department of Computer Science, Aalto University
[2]Obesity Research Unit, Research Programs Unit, Clinical and Molecular Metabolism, University of Helsinki
[3]Department of Internal Medicine, Helsinki University Hospital
[4]Department of Gastrointestinal Surgery, Abdominal Center, Helsinki University Hospital and University of Helsinki
[5]HealthyWeightHub, Endocrinology, Abdominal Center, Helsinki University Hospital and University of Helsinki
onur.poyraz@aalto.fi
sini.heinonen@helsinki.fi

Abstract

Bariatric surgery enhances glucose metabolism, yet the detailed postprandial joint glucose and insulin responses, variability in individual outcomes and differences in surgical approaches remain poorly understood. To address this, we used hierarchical multi-output Gaussian process (HMOGP) regression to model the individual postprandial glucose and insulin responses and to estimate the average response curves from individual data. Our study included 44 patients with obesity who underwent either Roux-en-Y gastric bypass (RYGB) (n=24) or One-Anastomosis gastric bypass (OAGB) (n=20) surgery. The patients were followed up at 6th and 12th months after the operation, during which they underwent an oral glucose tolerance test (OGTT) and a mixed meal test (MMT). A marked reduction in glycaemia, an earlier glucose peaking time and increase and sharpening in the postprandial glucose and insulin responses were evident in both metabolic tests after the operations. MMT resulted in higher postprandial glucose and insulin peaks compared with OGTT and higher glucose and insulin responses were observed after RYGB compared with OAGB. Women and persons without T2DM had a healthier postprandial response before and after surgery. Computational modeling with HMOGP regression can be used to, in detail, predict the combined responses of patient cohorts to ingested glucose or a mixed meal, and help in assessing individual metabolic improvement after weight loss. This can lead to new knowledge in personalized metabolic interventions.

1 Introduction

The prevalence of obesity has increased enormously over the last decades. Over 1.8 billion people lived with overweight or obesity in 2017 (WHO factsheet). Obesity is associated with various diseases and metabolic problems such as type 2 diabetes (T2DM), dyslipidemia, cardiovascular diseases, and cancer (Zimmet et al., 2005; Guh et al., 2009).

Treating obesity is extremely difficult. While diet-induced weight loss strategies lead to modest results, bariatric surgery is the most effective treatment of obesity, leading to improved glucose tolerance already within days (Adams et al., 2012; Sjöström, 2013). Roux-en-Y gastric bypass (RYGB) has been the gold standard in bariatric surgery. One-Anastomosis gastric bypass (OAGB) emerged as a potentially more beneficial procedure for the resolution of T2DM (Almalki et al., 2018; Magouliotis et al., 2018), but recent randomized controlled trials have challenged this (Disse et al., 2014; Robert et al., 2019; Heinonen et al., 2023). Additionally, individual metabolic phenotypes of patients undergoing bariatric

*These authors contributed equally to this work.
†These authors contributed equally to this work

Preprint. Under review.

surgery, such as differential glucose response between sexes (Mauvais-Jarvis, 2018), have resulted in the need for understanding and modeling in detail the glycaemic responses in different patient cohorts before and after surgery.

Conventional methods for assessing glucose responses after oral glucose tolerance test (OGTT) and mixed meal test (MMT) have relied on averaging means of the patient responses for each individual separately. Previously used methods in assessing the results of these tests thus yield robust estimation of blood glucose regulation but lack detailed characteristics of the overall blood glucose/insulin response on the population level, and neglect individual differences. Additionally, OGTT is sparsely sampled and individual estimates may be missing from the available data. Artificial intelligence techniques to better understand blood glucose regulation have emerged in recent years (Li et al., 2020). For example, the Eindhoven Diabetes Education Simulator (E-DES) model has been successfully used for OGTT to develop personalized models of glucose and insulin sensitivity and to explore the heterogeneity in the responses (Erdős et al., 2021). In another study, methods quantifying glucose fluxes between tissues using tracers have been applied to create predictive models of glucose-insulin interactions in the analyses of MMT (Dalla Man et al., 2007). Zeevi et al. (2015) developed a machine-learning algorithm integrating blood parameters, dietary habits, anthropometrics, physical activity, and gut microbiota to estimate the glucose and insulin responses accurately. A Gaussian process has been previously used in modeling OGTT responses in patients with and without cystic fibrosis to provide measures of beta-cell function with quantified uncertainty (Garrish et al., 2023).

In this study, we developed hierarchical multi-output Gaussian process (HMOGP) regression, which is the combination of hierarchical Gaussian process (HGP) and multi-output Gaussian process (MOGP). The hierarchical Gaussian process (HGP) is beneficial when part of the data reveals different characteristics such as the considerable inter-individual variability usually observed in postprandial glucose and insulin responses (Park and Choi, 2010). On the other hand, the multi-output Gaussian process (MOGP) is able to deal with multiple correlated outputs (such as glucose and insulin dynamics) and to provide more accurate predictions than simply modeling these outputs separately (Álvarez et al., 2010; Liu et al., 2018; Moreno-Muñoz et al., 2018). HMOGP allows us (1) to model the insulin and glucose response together via multi-output (2) while considering the individual level differences through a hierarchical structure. It also (3) quantifies uncertainty in predictions, making it suitable for datasets with noise or missing values, and (4) can model non-linearities and complex temporal dynamics in postprandial responses, providing more accurate predictions than simpler models (Williams and Rasmussen, 2006). Modeling both OGTT and MMT data before and after different types of bariatric surgery and between sexes or patients with or without T2DM in detail with HMOGP regression allows incorporating model uncertainty in a way that allows for a more detailed assessment of postprandial glucose and insulin responses. The goal is to apply the results into clinical use and to be able to select the best treatment for each patient. In this study we thus evaluated model outcomes to better understand the postprandial glucose and insulin levels after an OGTT and an MMT, considering the differences between the sexes and two types of bariatric surgery, providing a thorough analysis of postprandial response with an advanced technique.

2 Methods

2.1 Subjects

We included patients with obesity (n=44, aged 46.6 years with 14 men and 30 women,26 patients with obesity and 18 patients with obesity and T2DM, matched for age and diabetes status between the operation types), who were examined before, and at 6th and 12th months after bariatric surgery with either Roux-en-Y gastric bypass (RYGB; n=24, 8 men, 16 women, n=9 with T2DM), or One-Anastomosis gastric bypass (OAGB; n=20, 6 men, 14 women, n=9 with T2DM). 33% of men vs. 43% of women had T2DM (p=0.836). The subjects were recruited from Helsinki University Hospital, through the Department of Gastrointestinal Surgery. The full randomized clinical trial is registered at clinicaltrials.gov with no. NCT02882685 and described in detail in Saarinen et al. (2019) and Heinonen et al. (2023). Written informed consent was obtained from all participants. The study protocol was designed and performed according to the principles of the Helsinki Declaration and approved by the Ethical Committee of the Helsinki University Central Hospital.

2.2 Bariatric surgery

In RYGB, the gastric pouch was created with one horizontal 45 mm and two vertical 60 mm staplers. The length of the biliary limb was 80 cm and that of the alimentary limb 130 cm. In OAGB, a tubular gastric pouch was created using 60 mm staplers along a 38Fr bougie starting at the crow's foot with a horizontal 45 mm stapler, and the omega loop being 210 cm long. The length of the bypasses were standardized between the procedures to allow for equal comparison. A 210 cm bioliopancreatic limb in OAGB and 80 cm biliopancreatic and 130 cm alimentary limbs in RYGB were chosen to obtain equally long bypassed intestine in both groups (Saarinen et al., 2019).

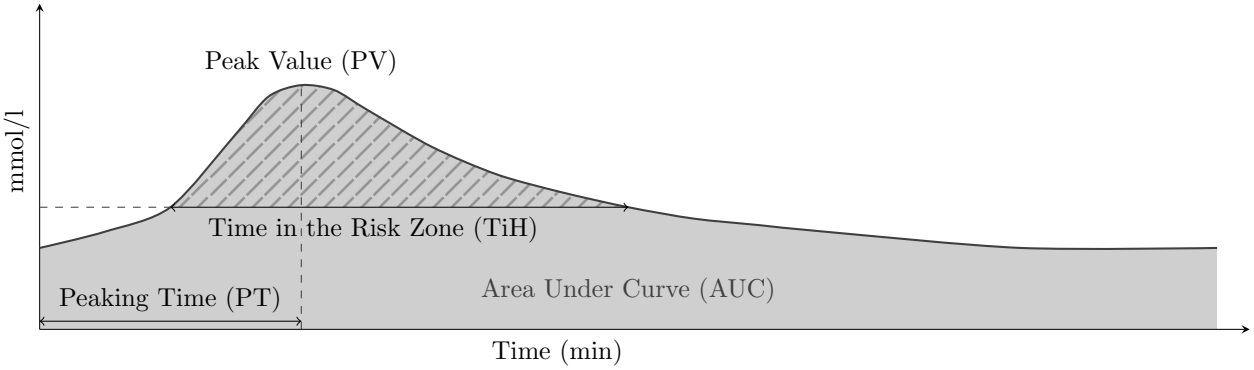

Figure 1 | Definition of the metrics evaluated in the experiments. Peaking Time (PT) and Time in the Risk Zone (TiH; Hyperglycaemia for glucose > 7.0mmol/l and Hyperinsulinemia for insulin > 50mmol/l) is represented in minutes, Peak Value (PV) represented in mmol/l, and Area Under Curve (AUC) represented in mmol/l*min.

2.3 Clinical examinations and body composition

Weight and height were measured after an overnight fast in light clothing. Whole body composition was measured by Dual-energy X-ray absorptiometry (DEXA) using a Lunar Prodigy whole bodyscanner (GE Medical Systems, Madison, WI).

2.4 Analytical blood samples

Fasting laboratory tests including blood count, Hba1c, plasma glucose and insulin and lipids were performed as previously described (Heinonen et al., 2015).

2.5 Mixed meal test (MMT) and oral glucose tolerance test (OGTT)

Glucose metabolism was measured after an overnight fast with a 3-hour oral glucose tolerance test (OGTT, 75 g of glucose), with time points 0 (before the ingestion), 30, 60, 120 and 180 min. We performed a 6-hour Mixed Meal Test (MMT) on a separate day, where a fasting blood sample was collected before ingesting the liquid meal of 2620 kJ (627 kcal) with a balanced distribution of fat (24 g), carbohydrates (76 g) and protein (24 g) (Resource® 2.5 Compact, Nestle Health Science), with post-meal samples taken at 0 min (before the ingestion), 15, 30, 60, 120, 180, 240 and 360 min for measuring glucose and insulin.

2.6 Data features

Each patient underwent both OGTT and MMT tests across three different visits; once preoperatively and then at 6th and 12th months postoperatively. Six patients missed the baseline OGTT visit, while 10 and 6 missed the 6th month and 12th month visits, respectively. In MMT, 4 and 5 patients missed the 6th and 12th month visits, respectively. Additionally, 3% of the overall data was missing due to vomiting or nausea, which interrupted the test.

2.7 Statistical method

Blood glucose and insulin evolve as a function of time. Here, we model them using a Gaussian process which is a continuous stochastic process and can be considered a probability distribution over functions (MacKay et al., 1998; Williams and Rasmussen, 2006). The standard Gaussian process regression is defined as:

$$\boldsymbol{y} \sim \mathcal{N}\left(f(t), \sigma I\right), \tag{1}$$

where $\boldsymbol{y} \in \mathbb{R}^T$ are the observation points, $t \in \{1, \ldots, T\}$ the input locations, and σ the measurement error. The function $f(t)$ is defined as the Gaussian process $f(t) \sim \mathcal{GP}(0, \mathbf{K})$ with kernel matrix $\mathbf{K}$. However, applying this approach directly to our problem is not straightforward. First, we know that glucose and insulin responses are strongly correlated, and applying Gaussian process regression on them separately would miss this correlation. Therefore, we propose to use Multi-Output Gaussian Process regression (Álvarez et al., 2010; Liu et al., 2018; Moreno-Muñoz et al., 2018), which is able calculate the cross-covariance between functions and are the proper choice for modeling insulin

and glucose together. If we define $\boldsymbol{f} = [f_{\text{glucose}}, f_{\text{insulin}}]$:

$$f_{\text{glucose}}(t) = \mathbf{L}_{11}\hat{f}_{\text{glucose}}(t) \tag{2}$$

$$f_{\text{insulin}}(t) = \mathbf{L}_{21}\hat{f}_{\text{glucose}}(t) + \mathbf{L}_{22}\hat{f}_{\text{insulin}}(t) \tag{3}$$

where $\hat{f}_{\text{glucose}}, \hat{f}_{\text{insulin}} \in \mathbb{R}^T$ are independent GPs and $\mathbf{L}$ is the Cholesky factor matrix of the corresponding correlation matrix $\mathbf{C}$, then $\boldsymbol{f} \in \mathbb{R}^{T\times D}$, where D is the output dimension (glucose, insulin) has the multi-output GP distribution. However, the challenge of the data is not limited to the output correlation. The second issue is that individuals have slightly different blood glucose and insulin responses. Hierarchical Gaussian process regression modeling can solve this issue by learning the population average response curve and individual deviations from the average response separately (Park and Choi, 2010). Let $\boldsymbol{f}_n(t)$ denote the response curve for a single patient, $\boldsymbol{f}^{\text{population}}(t)$ the average response curve across all patients, and $\boldsymbol{f}_n^{\text{patient}}(t)$ the deviation of the patient from the average response. Then hierarchical GP can be represented as:

$$\boldsymbol{f}_n(t) = \boldsymbol{f}^{\text{population}}(t) + \boldsymbol{f}_n^{\text{patient}}(t) \tag{4}$$

where $\boldsymbol{f}^{\text{population}}, \boldsymbol{f}_n^{\text{patient}} \in \mathbb{R}^{T\times D}$ have multi-output Gaussian process distributions. We apply the same hierarchical approach to model the constant terms for fasting glucose and insulin, as follows:

$$\boldsymbol{\mu}_n = \boldsymbol{\mu}^{\text{population}} + \boldsymbol{\mu}_n^{\text{patient}} \tag{5}$$

where $\boldsymbol{\mu}_n$ is fasting glucose and insulin for a single patient, $\boldsymbol{\mu}^{\text{population}}$ corresponds to the normally distributed population average of fasting glucose and insulin, and $\boldsymbol{\mu}_n^{\text{patient}}$ denotes the normally distributed individual deviation from the population average.

Overall, we modeled the data using the Hierarchical Multi-Output Gaussian process (HMOGP), where hierarchy allows us to consider the deviations of individual responses, and multi-output models the correlation of insulin and glucose response. Let the whole data be denoted by $\boldsymbol{y} \in \mathbb{R}^{N\times T\times D}$, where N is the total number of patients, T is the number of time points and $D = 2$ refers to the two possible outputs (glucose, insulin). If we index patient by n, time by t, and output by d, the blood glucose and insulin level $\boldsymbol{y}_{n,t}$ of patient n at time t can be represented as

$$\boldsymbol{y}_{n,t} \sim \mathcal{N}\left(\boldsymbol{f}_n(t), \Sigma\right), \tag{6}$$

where Σ is the diagonal measurement error matrix, and the latent function $\boldsymbol{f}_n$ is formulated as

$$\boldsymbol{f}_n(t) = \boldsymbol{\mu}^{\text{population}} + \boldsymbol{\mu}_n^{\text{patient}} + \boldsymbol{f}^{\text{population}}(t) + \boldsymbol{f}_n^{\text{patient}}(t). \tag{7}$$

We applied this model separately to the different visits (Baseline, 6th month, 12th month) and tests (OGTT, MMT). The only shared parameter across these models was the measurement error. For comparisons by operation, sex, and T2DM, we divided the dataset accordingly and modeled them separately. Further details of the model parameters and priors, along with the Stan code of the model can be found in Appendix A.

Stan software (Carpenter et al., 2017) was used to draw samples from the posterior distributions using the Markov Chain Monte Carlo inference, which we used to calculate Bayesian credible intervals (CI) and p-values Gelman et al. (2013). Furthermore, we used four metrics to investigate the characteristics of the postprandial glucose and insulin responses: peak value (PV), area under the curve (AUC), peaking time (PT) and time in the risk zone (TiH; Hyperglycaemia for glucose $>$ 7.0mmol/l and Hyperinsulinemia for insulin $>$ 50mmol/l). These metrics are illustrated in Figure 1. In the clinical analyses non-normally distributed variables were log10 transformed before the parametric analyses. Differences at baseline between the groups were analysed by Student's T-tests and between visits with generalized linear mixed modelling adjusting for sex, T2DM and operation type (Stata Statistical software vs. 7.0). These results are presented as means and 95% confidence intervals (CI).

3 Results

First, using hierarchical multi-output Gaussian process (HMOGP) regression, which is suitable for longitudinal data, we investigated the glucose and insulin responses in all patients following an oral glucose tolerance test (OGTT) and a mixed meal test (MMT). Both tests had similar amounts of carbohydrates ingested, but in MMT, glucose was combined with protein and fats. Figure B.1 and Figure B.2 shows the response by individuals, which validates the model fit for different persons. Note that Figure B.1 and Figure B.2 shows only the patients with full observations while the model was fitted using all the patients.

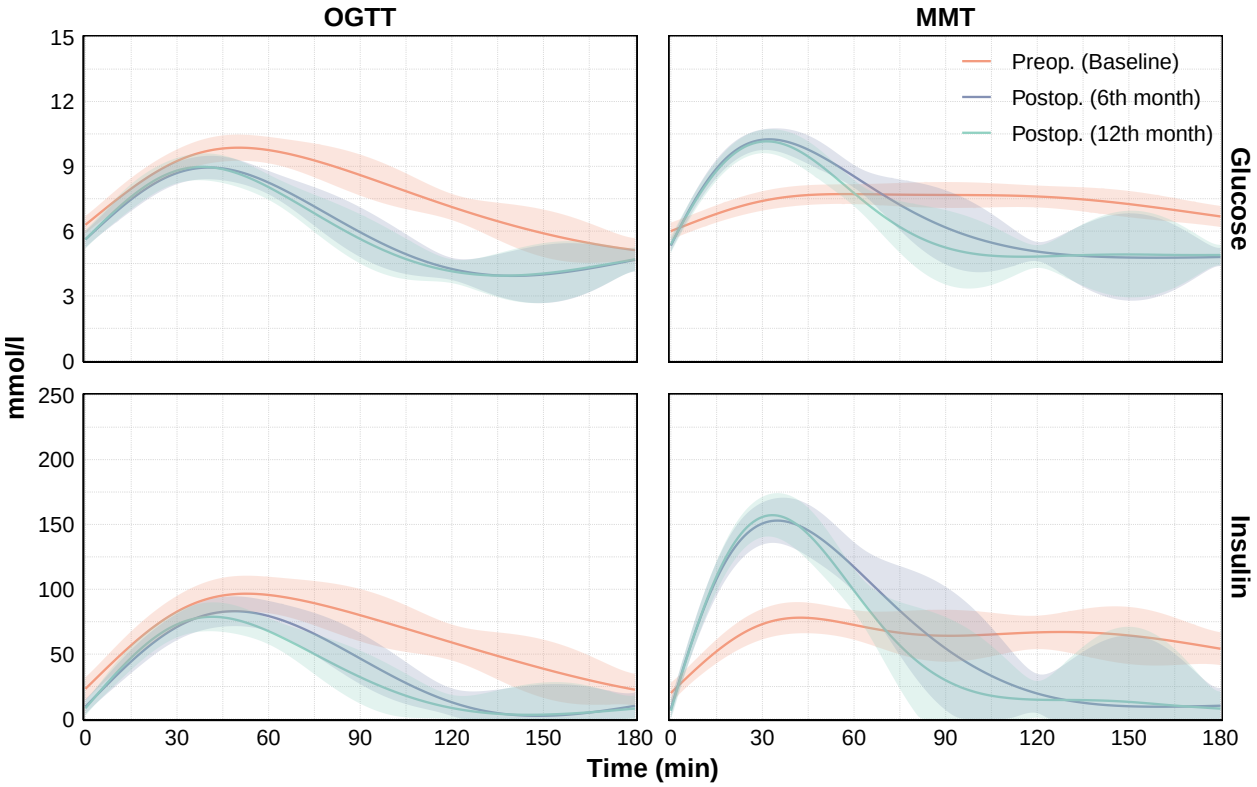

Figure 2 | The comparison of average glucose and insulin responses in different visits (Baseline, 6th month, and 12th month) within OGTT and MMT tests.

3.1 Glucose and insulin responses sharpen post-surgery in OGTT and MMT

From baseline to 12 months post-surgery, the glucose-insulin response improved in both tests (Figure 2). During the OGTT, the mean AUCs for glucose and insulin concentrations significantly decreased from baseline to 6th and 12th months (Table F.3). Peak values (PV) of both glucose and insulin were reduced by 0.9 mmol/l and by 18mmol/l from baseline to 12th month, respectively (Table F.2). The time to reach peak glucose (PT) occurred 12 minutes earlier at 12th month (51 min vs. 39 min) and 11 minutes for insulin (54 min vs. 43 min) compared with the baseline (Table F.1). Time in hyperglycemia (TiH glucose) was 53 min reduced during the weight loss, already bringing about large metabolic benefits (Table F.4). Overall, the OGTT results demonstrate a sharpened and significantly earlier glucose and insulin response with lower peak values following bariatric surgery (Figure 2).

In the MMT, both glucose and insulin AUCs showed a significant reduction from baseline to 12 months (Table F.3). Unlike in the OGTT, the peak glucose value (PV) significantly increased by 2.4 mmol/l (7.8 to 10.2) and the peak insulin value increased by 78 mmol/l (80 to 158) over 12 months (Table F.2). The peak time (PT) for glucose response occurred 48 minutes earlier (78 min to 32 min), and for insulin, it was 11 minutes earlier (45 min to 34 min) from baseline to 12th month. (Table F.1). Additionally, there was a total reduction of 83 minutes in TiH glucose between baseline and 12th month (Table F.4). These findings indicate a sharper and more pronounced glucose-insulin response, with significantly higher peak values and earlier peak times after bariatric surgery in MMT (Figure 2).

3.2 Higher postprandial glucose-insulin response in MMT vs. OGTT

OGTT and MMT evaluate patients' metabolic status through differential ingestion of macro-nutrients between the tests. We next analyzed the average postprandial response in glucose and insulin, comparing MMT and OGTT by including similar follow-up times of 180 minutes in both tests (Figure 3). Baseline responses in peak glucose and peak insulin (PV) were higher after OGTT than MMT, but other baseline metrics did not differ (Appendix F). Postoperatively at the 6th and 12th months, glucose and insulin responses (AUC, PV, and PT) were all significantly enhanced in MMT compared with OGTT (Appendix F). TiH for glucose did not differ between the tests during the weight loss. While both tests are performed in the same individuals and on following days, these differences could be attributed to the variable

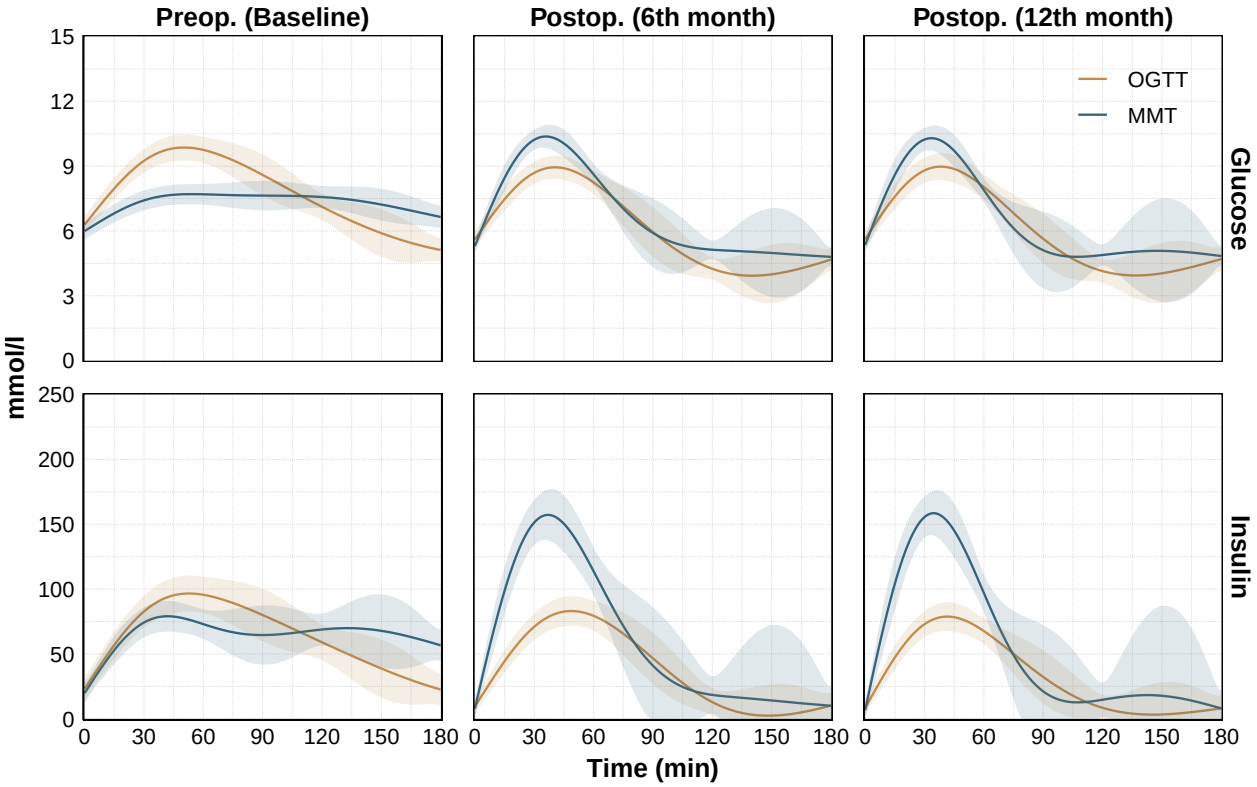

Figure 3 | The comparison of average glucose and insulin responses by OGTT and MMT test in different visits.

absorption of glucose in combination with other macro-nutrients, and to an additional insulin stimulus originating from proteins and fats included in the MMT.

3.3 Glucose-insulin response is higher and longer after RYGB than OAGB

In this part of the study, we modeled RYGB (n=24) and OAGB (n=20) groups separately. Figure 4 and Figure 5 show population comparison for OGTT and MMT tests, respectively. At baseline, the RYGB and OAGB groups had comparable glucose and insulin responses in both OGTT and MMT, except for a higher insulin peak in MMT for the RYGB group (Table F.2). In the OGTT, the RYGB group showed a trend towards a larger AUC for glucose compared to the OAGB group (p=0.09) at the 12th month, and had a significantly larger AUC for insulin at the 6th month (Table F.3). The peak glucose value (PV) for RYGB vs. OAGB at 12th month was higher (10.0 mmol/l vs. 7.8 mmol/l). For insulin, the RYGB group had a higher peak at the 6th month (104 mmol/l vs. 69 mmol/l), and a trend towards it at the 12th month (87 vs. 71 mmol/l, p=0.062, Table F.2). The peaking time shows no difference between operations (Table F.1)). Time in hyperglycemia (TiH) was longer in RYGB vs. OAGB group at 12th month, with 70 min vs. 47 min (Table F.4) but over the full weight-loss period the mean TiH reduction was similar between RYGB and OAGB (55 min vs.58 min).

In the MMT, the enhanced glucose and insulin responses in the RYGB group compared with the OAGB group were even more pronounced, with significantly higher peak values (PV) and areas under the curve (AUC) for both glucose and insulin at 6th and 12th months (Table F.2, Table F.3). Peak times for glucose and insulin were similar between the groups at all time points (Table F.1). Interestingly, the RYGB group experienced more time in hyperglycemia (TiH) (83 min vs. 53 min) at the 6th month and a trend towards it (69 min vs. 54 min, p=0.054) at the 12th month compared with the OAGB group (Table F.4). This may be partly due to the higher peak glucose levels observed in RYGB. Over the 12 months, the reduction in TiH was 64 minutes for RYGB and 82 minutes for OAGB.

Overall, RYGB surgery induces a more pronounced glucose and insulin response in both tests, particularly in the MMT, compared with OAGB. Peaking times for glucose and insulin remained similar between the two surgeries. The pronounced peak values and AUC in the RYGB group may drive the differences between MMT and OGTT in the postprandial response after surgery.

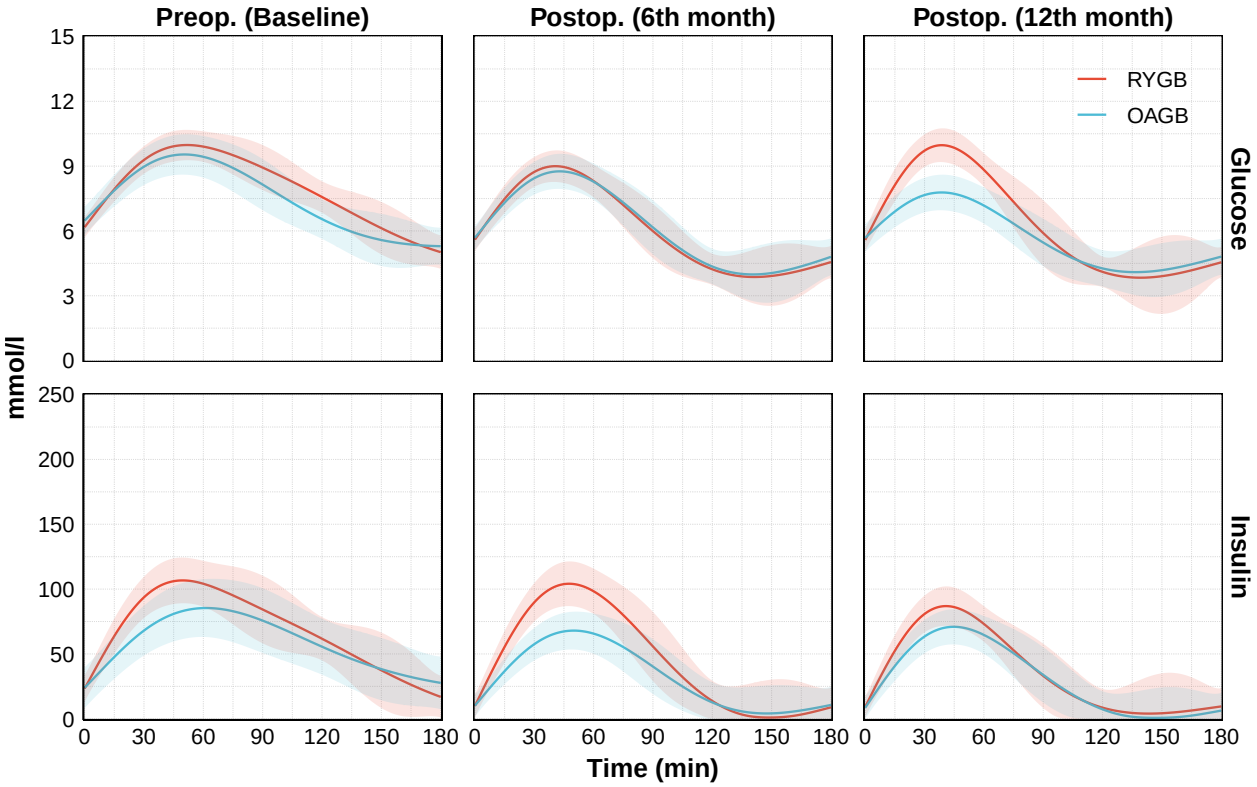

Figure 4 | The comparison of average glucose and insulin response of the patients with Roux-en-Y gastric bypass (RYGB) and One-Anastomosis gastric bypass (OAGB) operation in OGTT test.

3.4 Higher postprandial glucose but not insulin response in men vs. women

Next, we modeled women (n=30) and men (n=14) as different groups. Figure E.1 and Figure E.2 show population comparison for OGTT and MMT tests, respectively. In the OGTT, men exhibited higher peak values (PV) of glucose and insulin, and a higher AUC for insulin compared with women at baseline (Appendix F). Men consistently had higher postprandial peak glucose response at all visits and a higher glucose AUC at the 12th month (Table F.2). At the 12th month, men had a later peaking time (PT) for both glucose and insulin (Table F.1), spent more time in hyperglycemia (TiH), and had a smaller reduction of 31 minutes in hyperglycaemic time compared with 62 minutes reduction in women over the entire weight-loss period (Table F.4).

In the MMT, men and women showed similar baseline characteristics (Figure E.2). Men exhibited higher glucose and insulin AUCs at the 6th month along with higher glucose PV at the 6th and 12th months compared with women (Table F.2, and Table F.3). At the 6th month the peaking times (PT) in glucose and insulin occurred later with men (Table F.1) and men also spent more time in hyperglycemia (TiH) at 6th month, but the sexes had similar improvement in TiH during the entire weight loss (Table F.4).

3.5 Higher postprandial glucose but lower insulin response in T2DM vs non-T2DM

While T2DM is known to alter glucose metabolism, we additionally evaluated the postprandial glucose and insulin responses between persons with T2DM (n=18) separately from those without (n=26) (Appendix D). As expected, at baseline and at all visits in OGTT, persons with T2DM had higher PV and mean glucose AUC, later peaking time and longer TiH in glucose, and later peak time and lower PV in insulin (Appendix F). In MMT, glucose PV and mean AUC were higher and TiH longer with T2DM at all timepoints, and PV of insulin at 12 months lower than in persons without T2DM (Appendix F). Both groups improved in their glucose and insulin responses during the weight loss.

3.6 Metabolic features in all patients improve during weight loss

At baseline, both RYGB and OAGB groups had similar metabolic features. Women had higher fat percentage than men, and persons with T2DM had higher Hba1c and fasting plasma glucose than persons without T2DM. During the weight

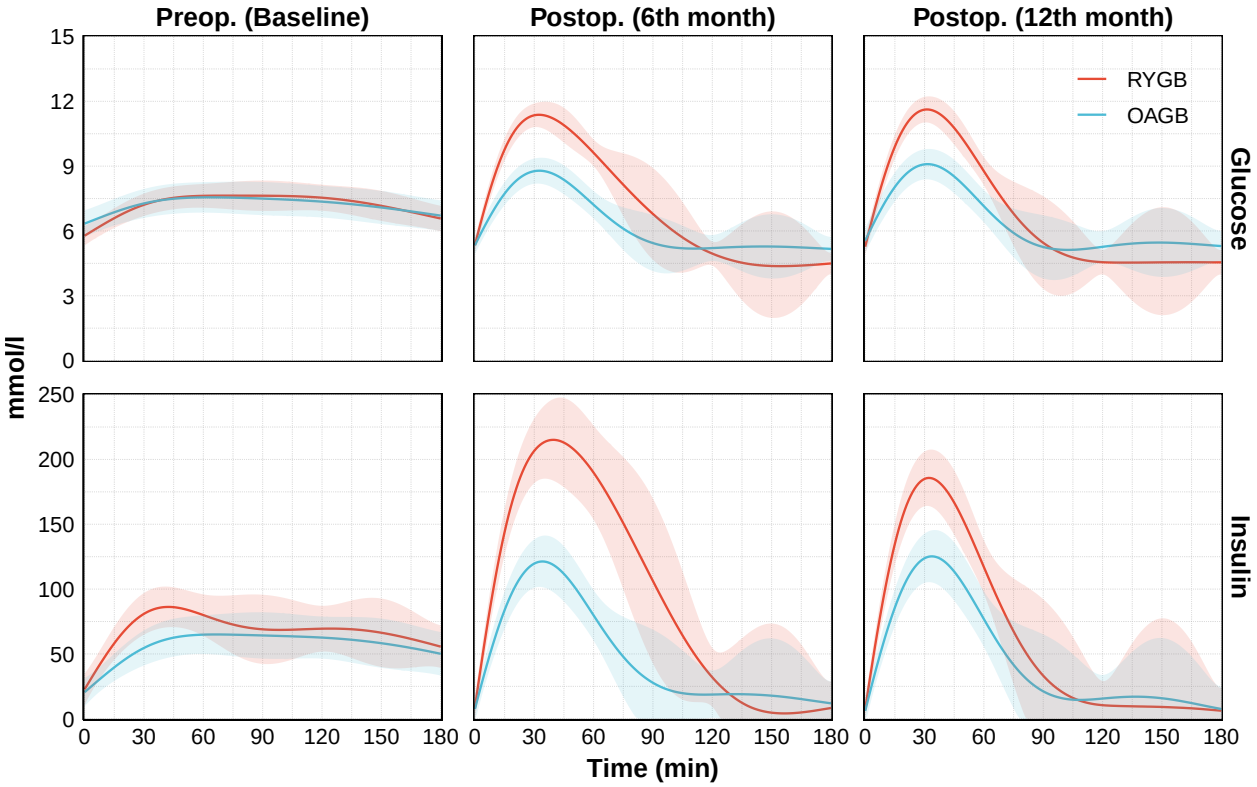

Figure 5 | The comparison of average glucose and insulin response of the patients with Roux-en-Y gastric bypass (RYGB) and One-Anastomosis gastric bypass (OAGB) operation in MMT test.

loss, body weight, fat kilograms, fat percentage, fasting glucose, fasting insulin, and lipid levels improved significantly in all groups (Table G.1). A slightly more prominent decrease in Hba1c in favor of OAGB vs. RYGB was observed, and HDL-cholesterol, fat kilograms, and fat percentage improved better in men vs. women. In persons with T2DM weight, Hba1c and fasting glucose improved more than in those without T2DM. (Table G.1).

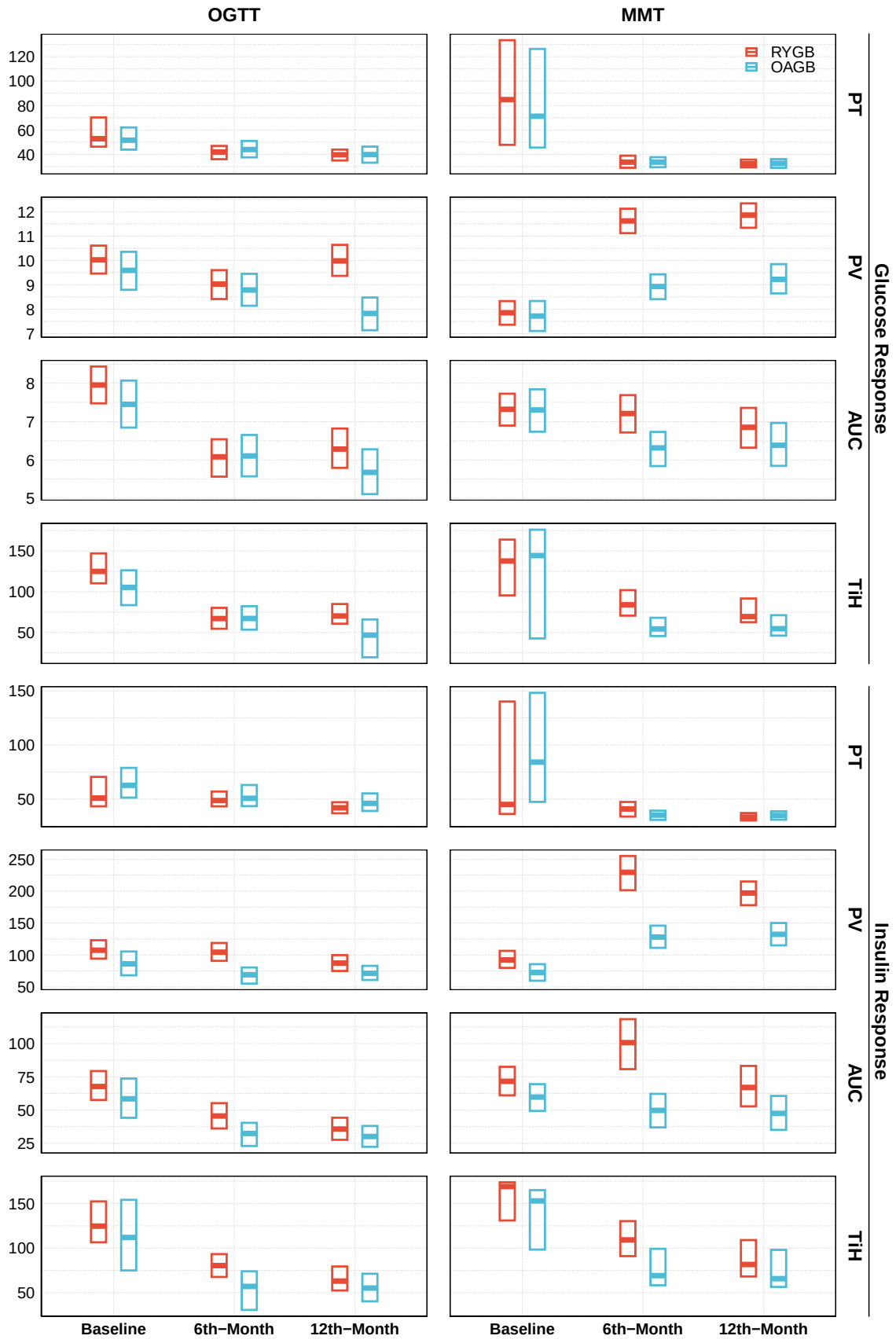

Figure 6 | Visualization of the metrics for operation comparison. See Appendix F for the 95 % CIs and p-values.

4 Discussion

We used hierarchical multi-output Gaussian process (HMOGP) regression to present a novel method suitable for blood glucose and insulin analyses in OGTT and MMT and reveal alterations in responses between two types of bariatric surgery and between sexes. Biologically, this study reveals sharper and earlier glucose-insulin responses and earlier restoration to baseline levels in OGTT and in MMT after bariatric surgery, higher postoperative glucose-insulin peaks in MMT than in OGTT and in RYGB than in OAGB. In addition, we present metabolic differences in glycaemic response in men compared with women and in T2DM compared with non-T2DM. This approach can be used for modeling postprandial glucose-insulin responses in detail in different patient groups for personalized treatment strategies, allowing for new means to understand and improve individual glycaemic responses in metabolic conditions.

Both OGTT and MMT provide a tool to assess the pancreatic beta-cell response that includes activation of the gut-related insulin stimulating hormones. OGTT is the standard method for assessing glucose intolerance and T2DM but MMT provides a more comprehensive physiological stimulus due to glucose in combination with protein and fats that can also activate insulin secretion from pancreas (Cersosimo et al., 2014). Our study proposes Hierarchical Multi-Output Gaussian Process (HMOGP) regression machine learning as suitable for in detail modelling postprandial glucose-insulin data in both tests. Evaluating different metrics of postprandial responses using computational modeling is crucial, as relying solely on AUC may overlook beneficial metabolic changes, especially given the blunted responses often seen in obesity. Previous studies have used Gaussian process for modeling OGTT responses in patients with and without cystic fibrosis (Garrish et al., 2023) but not in MMT nor in the context of obesity or weight loss. Traditional linear regression models or simple curve-fitting approaches assume independence between glucose and insulin, and fail to capture individual variability. Non-hierarchical Gaussian processes do not handle individual variations as effectively as the hierarchical structure in HMOGP (Alvarez and Lawrence, 2011)(Williams and Rasmussen, 2006). Additionally, fixed-effect models like ANOVA, or simpler mechanistic models, cannot accommodate individual-to-population hierarchy and multi-output dependencies. Our HMOGP method will allow a more granular understanding of how a patient compares with the population in terms of the insulin and glucose response after surgery. The additional advantages are suitability for the correlated structure of glucose and insulin dynamics, for datasets with noise or missing values (typical in OGTT and MMT), improved accuracy of the prediction and the ability to handle complex, multivariate data.

Biologically it is evident that the duration of the postprandial glucose-insulin peaks were significantly elevated and shortened after both metabolic tests, confirming enhanced insulin stimulus and improved glucose clearance from the circulation after the operations. Our results align with previous studies reporting that RYGB and vertical sleeve gastrectomy (VSG) surgeries lead to rapid increases in postprandial blood glucose levels paralleled by a surge in insulin secretion (Ferrannini and Mingrone, 2009). These metabolically beneficial changes may be at least partly explained by the renewed configuration of the gut after the operations. This includes a different nutrient absorption site with stimulation of the L-cells of the gut mucosa, and thus over 10 fold increase in the insulin-stimulating secretion of glucagon-like peptide-1 (GLP-1)(Cummings et al., 2007), and other gut hormones (Sandoval and Patti, 2023). Gut mucosa hyperplasia after the surgery favors absorption of glucose (Cavin et al., 2016) and pancreatic islets in mice studies seem to have an improved coordination to release insulin post-operatively (Akalestou et al., 2021), together contributing to an enhanced and a more rapid insulin secretion and glucose clearance from circulation.

The enhanced glucose-insulin response, earlier timing and quicker restoration of glucose levels post-operatively is highly beneficial, because hyperglycemia associates increased carotid artery media thickness, blood vessel endothelial dysfunction, cardiovascular risk factors, oxidative stress, inflammation and cognitive dysfunction (Di Giuseppe et al., 2023). Interestingly, earlier timing of the glucose-insulin peaks in OGTT also seem to indicate the effectiveness of the antidiabetic drugs (Tran et al., 2018) and reflect improved insulin sensitivity and secretion in T2DM (Wang et al., 2018b). Delayed glucose peaks in turn are related to pancreatic beta-cell dysfunction(Tran et al., 2018). In addition, the increasing complexity of the OGTT curve shape associates with improvement in glucose tolerance (Tura et al., 2011). These observations indicate metabolic benefits with a more complex, sharp, high peak-valued and earlier glucose-insulin responses. However, high glycaemic peaks after OGTT have also been connected with marks of atherosclerosis (Temelkova-Kurktschiev et al., 2000) and higher pulse pressure (Anan et al., 2008). High peaks in certain metabolic conditions could thus in some settings be also detrimental. Up to our knowledge no studies have assessed these parameters in context of MMT. The used modelling approach aligns with biologically meaningful results and thus provides reliable data for personalized glucose-insulin dynamics. The metabolic and predictive value of the sharp and early glucose-insulin peaks will gain more understanding in the future.

In the current study, a higher peak glucose-insulin response, thus larger AUC of the curve and longer time over 7.0 mmol/l glucose in RYGB are observed compared with OAGB, however, with similar peak times and restoration towards baseline levels in both operation types. This difference was especially pronounced after surgery in MMT. Earlier non-randomized trials, with different lengths of the bypassed intestine between the two operations, have resulted in indications of better glucose profile after OAGB than RYGB (Wang et al., 2018a). However, the few randomized clinical

trials (RCTs) with similar bypassed intestine lengths have demonstrated that RYGB and OAGB are metabolically equivalent at 1- and 2-year follow-ups (Heinonen et al., 2023; Robert et al., 2019). Results from the same RCTs indicate equal improvements in fasting glucose, Hba1c, and postprandial glucose and insulin AUCs in OGTT (calculated by linear trapezoidal method) up to 1 year post-surgery (Heinonen et al., 2023) and glycaemic responses to reported carbohydrate intakes, measured by FreeStyle Libre during 14 days before and after RYGB and OAGB appear to be similar (Ashrafi et al., 2021).

Postprandial glucose and insulin responses in OGTT or in MMT between RYGB and OAGB have not been explored, with no studies by HMOGP modeling. The pronounced response in RYGB vs. OAGB may be attributed to anatomical differences between the operations, with shorter route for the nutrients to reach the same areas in the gut. This leads to quicker absorption of glucose, followed by an increased insulin secretion in RYGB vs. OAGB. However, due to the increased peak value in RYGB, glucose concentrations after MMT seem to remain longer above the hyperglyceamic range. High glycaemic peaks may associate with atherosclerosis and hypertensive pulse pressure (Temelkova-Kurktschiev et al., 2000; Anan et al., 2008) but previous studies have nevertheless found better improvement in hypertension and less use of antihypertensive medications after RYGB vs. OAGB in 1 year follow-up (Heinonen et al., 2023). The postprandial increase in the RYGB curve also quickly restores, which can be seen as a metabolically healthy phenomenon. Reduction in overall glycaemia after surgery is nevertheless highly beneficial and the effects of bariatric surgery metabolically outstanding (Sinclair et al., 2018). The long-term effects of this increased peak of glucose and insulin stimulus from pancreas after RYGB can in future be metabolically relevant.

Our study reveals that in obesity and after bariatric surgery, men exhibit higher peak glucose in OGTT compared to women, and higher peak glucose and insulin post-operatively in both OGTT and MMT in addition to longer TiH, suggesting a potentially more unhealthy profile for men throughout obesity and weight loss. Typically, women have lower fasting plasma glucose, higher 2-hour glucose, and greater increases in 2-hour glucose following OGTT than men, though HbA1c levels are comparable between sexes (Sicree et al., 2008) Insulin sensitivity is generally greater in women due to higher glucose disposal by skeletal muscle (Nuutila et al., 1995) and women possibly also have higher postprandial insulin and C-peptide concentrations despite similar plasma glucose after a MMT than men (Basu et al., 2006).

While some studies suggest higher postprandial insulin in women, research on obesity is sparse, with older studies indicating that men have higher peak glucose at 1 hour during OGTT, but women surpass them at 2-3 hours (Young et al., 1979). Recent data shows that bariatric surgery leads to similar T2DM resolution and outcomes between sexes, though AUC insulin during OGTT in men predicts better weight loss (Risi et al., 2022) (Shu et al., 2024). These findings suggest women may have sharper and quicker glucose-insulin responses post-surgery, though these differences may not be clinically significant. To our knowledge, previous studies have not compared OGTT and MMT responses before and after bariatric surgery between the sexes, nor with HMOGP modelling. We confirm that in obesity there is blunted glucose-insulin response in both sexes in MMT, and a possibly unhealthier glucose profile for men in OGTT, and after the operation, women present a sharper but lower glucose-insulin peaks in both tests indicating sex-related advantages in glucose-insulin responses post-operatively.

Bariatric surgery results into excellent rates of T2DM remission (Courcoulas et al., 2024) but its effects on postprandial glycemia between persons with or without T2DM are not yet well characterized. Some studies suggest less weight loss in persons with T2DM (Rebelos et al., 2023) but do not assess postprandial glycaemic response. In our study, individuals with T2DM lost more weight and showed better metabolic improvements but had higher glucose, lower insulin responses, and a flatter curve at all time points compared to non-diabetic individuals. This altered response reflects significant changes in glucose and insulin dynamics in T2DM, warranting more individualized characterization of postprandial glycemic responses.

The strengths of this study include the standardized OGTT and MMT measurements conducted on the same individuals undergoing bariatric surgery, with follow-up extending to 6th and 12th months. The used cohort and its subgroups are representative of a general population undergoing bariatric surgery (Heinonen et al., 2023; Saarinen et al., 2019) making the results generalizable. The comparisons between RYGB and OAGB are derived from a randomized controlled trial specifically designed to compare these procedures, using identical bypass limb lengths and equal stratification of patients by sex, age, and T2DM status. These factors enhance the reliability of comparisons between OGTT and MMT results. Additionally, the MMT's extended follow-up period of 360 minutes is a unique strength of this study. Assessing responses at multiple time points provides insights into the temporal dynamics of metabolic changes, and examining different subgroups enhances relevance by identifying specific patterns related to surgical procedures, gender differences, and T2DM. While a larger cohort and more balanced sex distribution could have allowed for a more detailed analysis, the design still provides valuable insights. A follow-up study with a larger separate dataset including participants from different ethnic backgrounds can validate our findings. It is also worth noting that OGTT and MMT were performed on consecutive days, which may introduce slight day-to-day variations in glucose-insulin responses.

The limitations of the HMOGP model itself can in general be its computationally intensive structure and knowledge needed to choose model parameters. These can be overcome by an expert to design the model for specific clinical use. The model also assumes that data can take any real value but in reality, glucose and insulin levels cannot go below 0. To handle this, we transformed the data into a logarithmic scale. Additionally, HMOGP can give a large number of predictions, because two separate models (one for the individual and one for the population) are being used. To manage this, we imposed a strong assumption on the individual model, ensuring that it stays near 0 unless there are significant differences from the population response.

5 Conclusions

Utilizing Hierarchical Multi-Output Gaussian Process (HMOGP) regression modeling to analyze postprandial OGTT and MMT responses presents a novel advanced approach to study postprandial glucose-insulin responses in obesity and in weight loss. The employed HMOGP regression is capable of estimating individual-level effects — the personalized treatment response — in addition to the effects at the population level while accounting for and correcting for measurement errors and thus improve accuracy in complex multivariate data. This method not only unveils differences between metabolic cohorts after bariatric surgery but a differential response between two operation types and sexes. This can lead to new knowledge in choosing the right patients for certain types of treatments, and to a more accurate modelling method for assessing OGTT and MMT responses in the clinic. HMOGP regression offers a versatile tool for investigating and predicting glycaemic responses in metabolic conditions, paving way for personalized interventions of metabolic health.

Acknowledgments

We thank the participants for their invaluable time and effort. We also thank the study nurses, dieticians, and laboratory personnel for their help.

Funding

The study was supported by the Research Council of Finland (272376, 266286, 314383, and 335443 to KHP, 314457 to AJ, 338417 to SH), the Finnish Medical Foundation (KHP, SH and AJ), the Finnish Diabetes Research Foundation (SH and KHP), the Orion Foundation (SH), the Novo Nordisk Foundation (NNF10OC1013354, NNF17OC0027232, and NNF20OC0060547 to KHP. NNF23SA0083953 for SH), the Paulo Foundation (SH), the Gyllenberg Foundation (KHP), Paavo Nurmi Foundation (SH), the Sigrid Juselius Foundation (KHP), Helsinki University Hospital Research Funds (SH, KHP, AJ), Government Research Funds (KHP, SH), the Research Council of Finland (Flagship programme: Finnish Center for Artificial Intelligence FCAI, and grants 352986, 358246 to PM) and EU (H2020 grant 101016775 and NextGenerationEU to PM).

Competing interests

The authors have no conflicts of interest to declare.

Data sharing statement

Individual participant data are not directly available but may be available after study close upon reasonable request from the authors. According to the General Data Protection Regulation of the European Union (679/2016), the principles of data protection should apply to any information concerning an identified or identifiable natural person and that personal data which have undergone pseudonymization, which could be attributed to a natural person by the use of additional information should be considered to be information on an identifiable natural person. Thus, according to the GDPR, all pseudonymized data are considered personal data and cannot be published openly. Therefore, we are bound to the law and to the strict hospital policies, and are unable to share the data directly. However, the institutional (Helsinki and Uusimaa Hospital District) contact details for potential future data requests are as follows: `https://huspalvelu.microsoftcrmportals.com/fi-FI/`.

References

Adams TD, Davidson LE, Litwin SE, Kolotkin RL, LaMonte MJ, Pendleton RC, Strong MB, Vinik R, Wanner NA, Hopkins PN, et al. Health benefits of gastric bypass surgery after 6 years. Jama. 2012; 308(11):1122–1131.

Akalestou E, Suba K, Lopez-Noriega L, Georgiadou E, Chabosseau P, Gallie A, Wretlind A, Legido-Quigley C, Leclerc I, Salem V, et al. Intravital imaging of islet Ca2+ dynamics reveals enhanced β cell connectivity after bariatric surgery in mice. Nature Communications. 2021; 12(1):5165.

Almalki OM, Lee WJ, Chong K, Ser KH, Lee YC, Chen SC. Laparoscopic gastric bypass for the treatment of type 2 diabetes: a comparison of Roux-en-Y versus single anastomosis gastric bypass. Surgery for Obesity and Related Diseases. 2018; 14(4):509–515.

Álvarez M, Luengo D, Titsias M, Lawrence ND. Efficient multioutput Gaussian processes through variational inducing kernels. In: *Proceedings of the Thirteenth International Conference on Artificial Intelligence and Statistics* JMLR Workshop and Conference Proceedings; 2010. p. 25–32.

Alvarez MA, Lawrence ND. Computationally efficient convolved multiple output Gaussian processes. The Journal of Machine Learning Research. 2011; 12:1459–1500.

Anan F, Masaki T, Eto T, Fukunaga N, Iwao T, Kaneda K, Eshima N, Saikawa T, Yoshimatsu H. Postchallenge plasma glucose and glycemic spikes are associated with pulse pressure in patients with impaired glucose tolerance and essential hypertension. Hypertension Research. 2008; 31(8):1565–1571.

Ashrafi RA, Ahola AJ, Rosengård-Bärlund M, Saarinen T, Heinonen S, Juuti A, Marttinen P, Pietiläinen KH. Computational modelling of self-reported dietary carbohydrate intake on glucose concentrations in patients undergoing Roux-en-Y gastric bypass versus one-anastomosis gastric bypass. Annals of medicine. 2021; 53(1):1885–1895.

Basu R, Dalla Man C, Campioni M, Basu A, Klee G, Toffolo G, Cobelli C, Rizza RA. Effects of age and sex on postprandial glucose metabolism: differences in glucose turnover, insulin secretion, insulin action, and hepatic insulin extraction. Diabetes. 2006; 55(7):2001–2014.

Carpenter B, Gelman A, Hoffman MD, Lee D, Goodrich B, Betancourt M, Brubaker MA, Guo J, Li P, Riddell A. Stan: A probabilistic programming language. Journal of statistical software. 2017; 76.

Cavin JB, Couvelard A, Lebtahi R, Ducroc R, Arapis K, Voitellier E, Cluzeaud F, Gillard L, Hourseau M, Mikail N, et al. Differences in alimentary glucose absorption and intestinal disposal of blood glucose after Roux-en-Y gastric bypass vs sleeve gastrectomy. Gastroenterology. 2016; 150(2):454–464.

Cersosimo E, Solis-Herrera C, E Trautmann M, Malloy J, L Triplitt C. Assessment of pancreatic β-cell function: review of methods and clinical applications. Current diabetes reviews. 2014; 10(1):2–42.

Courcoulas AP, Patti ME, Hu B, Arterburn DE, Simonson DC, Gourash WF, Jakicic JM, Vernon AH, Beck GJ, Schauer PR, et al. Long-term outcomes of medical management vs bariatric surgery in type 2 diabetes. JAMA. 2024; 331(8):654–664.

Cummings DE, Overduin J, Foster-Schubert KE, Carlson MJ. Role of the bypassed proximal intestine in the anti-diabetic effects of bariatric surgery. Surgery for Obesity and Related Diseases. 2007; 3(2):109–115.

Dalla Man C, Rizza RA, Cobelli C. Meal simulation model of the glucose-insulin system. IEEE Transactions on biomedical engineering. 2007; 54(10):1740–1749.

Di Giuseppe G, Ciccarelli G, Soldovieri L, Capece U, Cefalo CM, Moffa S, Nista EC, Brunetti M, Cinti F, Gasbarrini A, et al. First-phase insulin secretion: can its evaluation direct therapeutic approaches? Trends in Endocrinology & Metabolism. 2023; 34(4):216–230.

Disse E, Pasquer A, Espalieu P, Poncet G, Gouillat C, Robert M. Greater weight loss with the omega loop bypass compared to the Roux-en-Y gastric bypass: a comparative study. Obesity surgery. 2014; 24:841–846.

Erdős B, van Sloun B, Adriaens ME, O'Donovan SD, Langin D, Astrup A, Blaak EE, Arts IC, van Riel NA. Personalized computational model quantifies heterogeneity in postprandial responses to oral glucose challenge. PLoS computational biology. 2021; 17(3):e1008852.

Ferrannini E, Mingrone G. Impact of different bariatric surgical procedures on insulin action and β-cell function in type 2 diabetes. Diabetes care. 2009; 32(3):514.

Garrish J, Chan C, Nychka D, Diniz Behn C. A Gaussian Process Model for Insulin Secretion Reconstruction with Uncertainty Quantification: Applications in Cystic Fibrosis. SIAM Journal on Applied Mathematics. 2023; p. S65–S81.

Gelman A, Carlin J, Stern H, Dunson D, Vehtari A, Rubin D. Bayesian Data Analysis. 3rd ed ed. United States: CreateSpace; 2013.

Guh DP, Zhang W, Bansback N, Amarsi Z, Birmingham CL, Anis AH. The incidence of co-morbidities related to obesity and overweight: a systematic review and meta-analysis. BMC public health. 2009; 9:1–20.

Heinonen S, Buzkova J, Muniandy M, Kaksonen R, Ollikainen M, Ismail K, Hakkarainen A, Lundbom J, Lundbom N, Vuolteenaho K, et al. Impaired mitochondrial biogenesis in adipose tissue in acquired obesity. Diabetes. 2015; 64(9):3135–3145.

Heinonen S, Saarinen T, Meriläinen S, Sammalkorpi H, Penttilä AK, Koivikko M, Siira P, Karppinen J, Säiläkivi U, Rosengård-Bärlund M, et al. Roux-en-Y versus one-anastomosis gastric bypass (RYSA study): weight loss, metabolic improvements, and nutrition at 1 year after surgery, a multicenter randomized controlled trial. Obesity. 2023; 31(12):2909–2923.

Li J, Huang J, Zheng L, Li X. Application of artificial intelligence in diabetes education and management: present status and promising prospect. Frontiers in public health. 2020; 8:521222.

Liu H, Cai J, Ong YS. Remarks on multi-output Gaussian process regression. Knowledge-Based Systems. 2018; 144:102–121.

MacKay DJ, et al. Introduction to Gaussian processes. NATO ASI series F computer and systems sciences. 1998; 168:133–166.

Magouliotis D, Tasiopoulou V, Tzovaras G. One anastomosis gastric bypass versus Roux-en-Y gastric bypass for morbid obesity: a meta-analysis. Clinical obesity. 2018; 8(3):159–169.

Mauvais-Jarvis F. Gender differences in glucose homeostasis and diabetes. Physiology & behavior. 2018; 187:20–23.

Moreno-Muñoz P, Artés A, Alvarez M. Heterogeneous multi-output Gaussian process prediction. Advances in neural information processing systems. 2018; 31.

Nuutila P, Knuuti MJ, Mäki M, Laine H, Ruotsalainen U, Teräs M, Haaparanta M, Solin O, Yki-Järvinen H. Gender and insulin sensitivity in the heart and in skeletal muscles: studies using positron emission tomography. Diabetes. 1995; 44(1):31–36.

Park S, Choi S. Hierarchical Gaussian process regression. In: *Proceedings of 2nd Asian conference on machine learning* JMLR Workshop and Conference Proceedings; 2010. p. 95–110.

Rebelos E, Moriconi D, Honka MJ, Anselmino M, Nannipieri M. Decreased weight loss following bariatric surgery in patients with type 2 diabetes. Obesity surgery. 2023; 33(1):179–187.

Risi R, Rossini G, Tozzi R, Pieralice S, Monte L, Masi D, Castagneto-Gissey L, Gallo IF, Strigari L, Casella G, et al. Sex difference in the safety and efficacy of bariatric procedures: a systematic review and meta-analysis. Surgery for Obesity and Related Diseases. 2022; 18(7):983–996.

Robert M, Espalieu P, Pelascini E, Caiazzo R, Sterkers A, Khamphommala L, Poghosyan T, Chevallier JM, Malherbe V, Chouillard E, et al. Efficacy and safety of one anastomosis gastric bypass versus Roux-en-Y gastric bypass for obesity (YOMEGA): a multicentre, randomised, open-label, non-inferiority trial. The Lancet. 2019; 393(10178):1299–1309.

Saarinen T, Meriläinen S, Koivukangas V, Pietiläinen KH, Juuti A. Prospective randomized controlled trial comparing the efficacy and safety of Roux-en-Y gastric bypass and one-anastomosis gastric bypass (the RYSA trial): trial protocol and interim analysis. Trials. 2019; 20:1–10.

Sandoval DA, Patti ME. Glucose metabolism after bariatric surgery: implications for T2DM remission and hypoglycaemia. Nature Reviews Endocrinology. 2023; 19(3):164–176.

Shu J, Zhu T, Xiong S, Liu T, Zhao Y, Huang X, Liu S. Sex dimorphism in the effect and predictors of weight loss after sleeve gastrectomy. Frontiers in Endocrinology. 2024; 14:1333051.

Sicree R, Zimmet P, Dunstan D, Cameron A, Welborn T, Shaw J. Differences in height explain gender differences in the response to the oral glucose tolerance test—the AusDiab study. Diabetic Medicine. 2008; 25(3):296–302.

Sinclair P, Docherty N, le Roux CW. Metabolic effects of bariatric surgery. Clinical chemistry. 2018; 64(1):72–81.

Sjöström L. Review of the key results from the Swedish Obese Subjects (SOS) trial–a prospective controlled intervention study of bariatric surgery. Journal of internal medicine. 2013; 273(3):219–234.

Temelkova-Kurktschiev TS, Koehler C, Henkel E, Leonhardt W, Fuecker K, Hanefeld M. Postchallenge plasma glucose and glycemic spikes are more strongly associated with atherosclerosis than fasting glucose or HbA1c level. Diabetes care. 2000; 23(12):1830–1834.

Tran S, Kramer CK, Zinman B, Choi H, Retnakaran R. Effect of chronic liraglutide therapy and its withdrawal on time to postchallenge peak glucose in type 2 diabetes. American Journal of Physiology-Endocrinology and Metabolism. 2018; 314(3):E287–E295.

Tura A, Morbiducci U, Sbrignadello S, Winhofer Y, Pacini G, Kautzky-Willer A. Shape of glucose, insulin, C-peptide curves during a 3-h oral glucose tolerance test: any relationship with the degree of glucose tolerance? American Journal of Physiology-Regulatory, Integrative and Comparative Physiology. 2011; 300(4):R941–R948.

Wang FG, Yan WM, Yan M, Song MM. Outcomes of Mini vs Roux-en-Y gastric bypass: a meta-analysis and systematic review. International Journal of Surgery. 2018; 56:7–14.

Wang X, Zhao X, Zhou R, Gu Y, Zhu X, Tang Z, Yuan X, Chen W, Zhang R, Qian C, et al. Delay in glucose peak time during the oral glucose tolerance test as an indicator of insulin resistance and insulin secretion in type 2 diabetes patients. Journal of diabetes investigation. 2018; 9(6):1288–1295.

Williams CK, Rasmussen CE. Gaussian processes for machine learning, vol. 2. MIT press Cambridge, MA; 2006.

Young RL, Fuchs RJ, Woltjen MJ, Cooperman MT. Glucose-insulin response to oral glucose in a healthy obese population. Diabetes. 1979; 28(3):208–212.

Zeevi D, Korem T, Zmora N, Israeli D, Rothschild D, Weinberger A, Ben-Yacov O, Lador D, Avnit-Sagi T, Lotan-Pompan M, et al. Personalized nutrition by prediction of glycemic responses. Cell. 2015; 163(5):1079–1094.

Zimmet P, Magliano D, Matsuzawa Y, Alberti G, Shaw J. The metabolic syndrome: a global public health problem and a new definition. Journal of atherosclerosis and thrombosis. 2005; 12(6):295–300.

A Modeling Details

We normalized the data in both time and value domains before the training, separately for insulin and glucose values. We used a fixed lengthscale parameters for all GPs, which is set to be $120/\sigma_{\text{time}}$, where σ_{time} is the standard deviation of the sample times. We used the Matern52 kernel for all GPs. The main difference between individual-level GPs and the population-level GPs was the prior value of the kernel variance. We used $InverseGamma(1, 1)$ distribution for the population level GPs, while for the individual level GPs, we used a stronger $InverseGamma(1, 0.1)$ distribution. This setup allowed the model to learn the shared behaviors with the population-level GPs while the individual-level GPs learned individual differences. For measurement error σ, we used $InverseGamma(1, 0.01)$ as a prior distribution. For $\boldsymbol{\mu}^{\text{population}}$, we used $\mathcal{N}(0, 1)$ as a prior distribution, and for $\boldsymbol{\mu}_n^{\text{patient}}$ we used $\mathcal{N}(\boldsymbol{\mu}^{\text{population}}, \sigma_n^{\text{patient}})$ as a prior distribution, where $\sigma_n^{\text{patient}} \sim InverseGamma(1, 0.5)$. The rest of the details can be found in the provided Stan code below.

```
functions {
  matrix gp_pred_multi_rng(array[] real x_pred,
                           array[] real x,
                           matrix y,
                           real lengthscale,
                           vector alpha,
                           matrix L_Omega){
    int N = rows(y);
    int D = cols(y);
    int N_pred = size(x_pred);
    matrix[D, D] corr = diag_pre_multiply(alpha, L_Omega)';
```

```
    matrix[N, D] y_U = y / corr;

    matrix[N, N] K = gp_matern52_cov(x, 1.0, lengthscale);
    matrix[N, N] L = cholesky_decompose(add_diag(K, rep_vector(1e-9, N)));

    matrix[N, N_pred] k_x_x_pred = gp_matern52_cov(x, x_pred, 1.0, lengthscale);
    matrix[N, N_pred] v_pred = mdivide_left_tri_low(L, k_x_x_pred);
    matrix[N_pred, N_pred] f_pred_cov = gp_matern52_cov(x_pred, 1.0, lengthscale)
                                        - v_pred' * v_pred;

    matrix[N_pred, D] f_pred;
    matrix[N_pred, D] f_pred_U;
    vector[N] K_div_y;
    vector[N_pred] f_pred_mu;
    for (d in 1:D) {
      K_div_y = mdivide_left_tri_low(L, y_U[, d]);
      K_div_y = mdivide_right_tri_low(K_div_y', L)';

      f_pred_mu = (k_x_x_pred' * K_div_y);

      f_pred_U[, d] = multi_normal_rng(f_pred_mu,
                                       add_diag(f_pred_cov,
                                                rep_vector(1e-9, N_pred)));
    }
    f_pred = f_pred_U * corr;
    return f_pred;
  }
}
data {
  int<lower=1> N_times;
  int<lower=1> N_times_pred;
  int<lower=1> N_patients;
  int<lower=1> N_dimensions;
  int<lower=1> N_visits;
  array[N_times] real times;
  array[N_times_pred] real times_pred;
  array[N_visits, N_patients, N_times, N_dimensions] int mask;
  array[N_visits, N_patients] matrix[N_times, N_dimensions] y;
  real<lower=0> lengthscale_common;
  real<lower=0> lengthscale_patient;
  real<lower=0> sigma_beta;
}
parameters {
  array[N_visits] vector[N_dimensions] mu_common;
  array[N_visits] vector<lower=0>[N_dimensions] sigma_patient;
  array[N_visits] matrix[N_patients, N_dimensions] mu_patient;
  array[N_visits] matrix[N_times, N_dimensions] eta_common;
  array[N_visits, N_patients] matrix[N_times, N_dimensions] eta_patient;

  array[N_visits] vector<lower=0>[N_dimensions] alpha_common;
  array[N_visits, N_patients] vector<lower=0>[N_dimensions] alpha_patient;

  array[N_visits] cholesky_factor_corr[N_dimensions] L_Omega_common;
  array[N_visits, N_patients] cholesky_factor_corr[N_dimensions] L_Omega_patient;

  vector<lower=0>[N_dimensions] sigma; // observation noise scale
}
transformed parameters {
  array[N_visits] matrix[N_times, N_dimensions] f_common;
```

```
  {
    matrix[N_times, N_times] K_common =
        gp_matern52_cov(times, 1.0, lengthscale_common);
    matrix[N_times, N_times] L_common =
        cholesky_decompose(add_diag(K_common, rep_vector(1e-9, N_times)));
    for (v in 1:N_visits) {
      f_common[v] = L_common * eta_common[v]
                    * diag_pre_multiply(alpha_common[v], L_Omega_common[v])';
    }
  }

  array[N_visits, N_patients] matrix[N_times, N_dimensions] f_patient;
  {
    matrix[N_times, N_times] K_patient =
        gp_matern52_cov(times, 1.0, lengthscale_patient);
    matrix[N_times, N_times] L_patient =
        cholesky_decompose(add_diag(K_patient, rep_vector(1e-9, N_times)));
    for (p in 1:N_patients) {
      for (v in 1:N_visits) {
        f_patient[v, p] = L_patient * eta_patient[v, p]
                          * diag_pre_multiply(alpha_patient[v, p],
                                              L_Omega_patient[v, p])';
      }
    }
  }

  array[N_visits, N_patients] matrix[N_times, N_dimensions] f;
  for (v in 1:N_visits) {
    for (p in 1:N_patients) {
      for (t in 1:N_times) {
        for (d in 1:N_dimensions) {
          f[v, p, t, d] = mu_patient[v, p, d]
                          + f_common[v, t, d]
                          + f_patient[v, p, t, d];
        }
      }
    }
  }
}
model {
  for (v in 1:N_visits) {
    mu_common[v] ~ normal(0, 1);
    sigma_patient[v] ~ inv_gamma(1, 0.5);
    for (d in 1:N_dimensions) {
      mu_patient[v, , d] ~ normal(mu_common[v, d], sigma_patient[v, d]);
    }
    to_vector(eta_common[v]) ~ normal(0, 1);
    L_Omega_common[v] ~ lkj_corr_cholesky(1);
    alpha_common[v] ~ inv_gamma(1, 1);
  }

  for (p in 1:N_patients) {
    for (v in 1:N_visits) {
      to_vector(eta_patient[v, p]) ~ normal(0, 1);
      L_Omega_patient[v, p] ~ lkj_corr_cholesky(1);
      alpha_patient[v, p] ~ inv_gamma(1, 0.1);
    }
  }
```

```
  sigma ~ inv_gamma(1, sigma_beta);

  for (v in 1:N_visits) {
    for (p in 1:N_patients) {
      for (t in 1:N_times) {
        for (d in 1:N_dimensions) {
          if (mask[v, p, t, d] == 1) {
            if (t == 1) {
              y[v, p, t, d] ~ normal(mu_patient[v, p, d], sigma[d] / 10);
              0 ~ normal(f_common[v, t, d], sqrt(pow(sigma[d], 2) * 0.495));
              0 ~ normal(f_patient[v, p, t, d], sqrt(pow(sigma[d], 2) * 0.495));
            }
            else {
              y[v, p, t, d] ~ normal(f[v, p, t, d], sigma[d]);
            }
          }
        }
      }
    }
  }
}
generated quantities {
  array[N_visits] matrix[N_dimensions, N_dimensions] Omega_common;
  array[N_visits, N_patients] matrix[N_dimensions, N_dimensions] Omega_patient;
  array[N_visits] matrix[N_times_pred, N_dimensions] f_common_pred;
  array[N_visits, N_patients] matrix[N_times_pred, N_dimensions] f_patient_pred;
  for (v in 1:N_visits) {
    Omega_common[v] = L_Omega_common[v] * L_Omega_common[v]';
    f_common_pred[v] = gp_pred_multi_rng(times_pred,
                                         times,
                                         f_common[v],
                                         lengthscale_common,
                                         alpha_common[v],
                                         L_Omega_common[v]);
    for (p in 1:N_patients) {
      Omega_patient[v, p] = L_Omega_patient[v, p] * L_Omega_patient[v, p]';
      f_patient_pred[v, p] = gp_pred_multi_rng(times_pred,
                                               times,
                                               f_patient[v, p],
                                               lengthscale_patient,
                                               alpha_patient[v, p],
                                               L_Omega_patient[v, p]);
    }
  }
  array[N_visits, N_patients] matrix[N_times_pred, N_dimensions] f_pred;
  array[N_visits, N_patients] matrix[N_times_pred, N_dimensions] y_pred;
  for (v in 1:N_visits) {
    for (p in 1:N_patients) {
      for (t in 1:N_times_pred) {
        for (d in 1:N_dimensions) {
          f_pred[v, p, t, d] = mu_patient[v, p, d]
                               + f_common_pred[v, t, d]
                               + f_patient_pred[v, p, t, d];
          y_pred[v, p, t, d] = normal_rng(f_pred[v, p, t, d], sigma[d]);
        }
      }
    }
  }
}
```

B Individual Responses

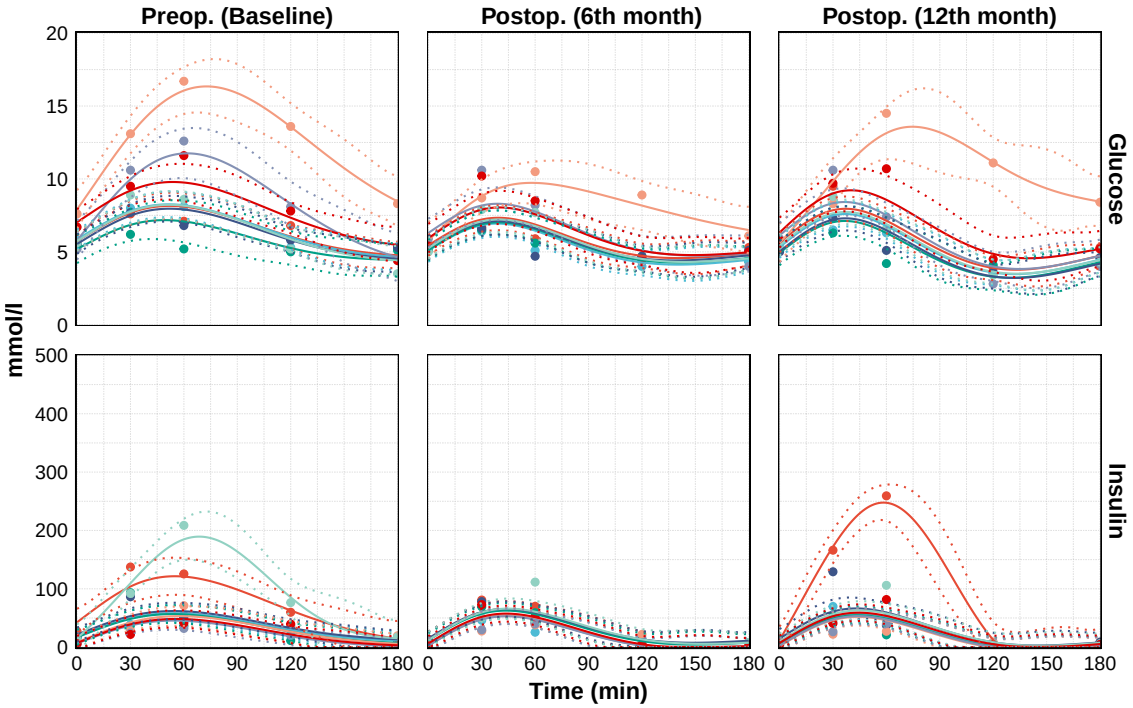

Figure B.1 | Response of the glucose and insulin levels and predicted model fit for different individuals with applied OGTT test.

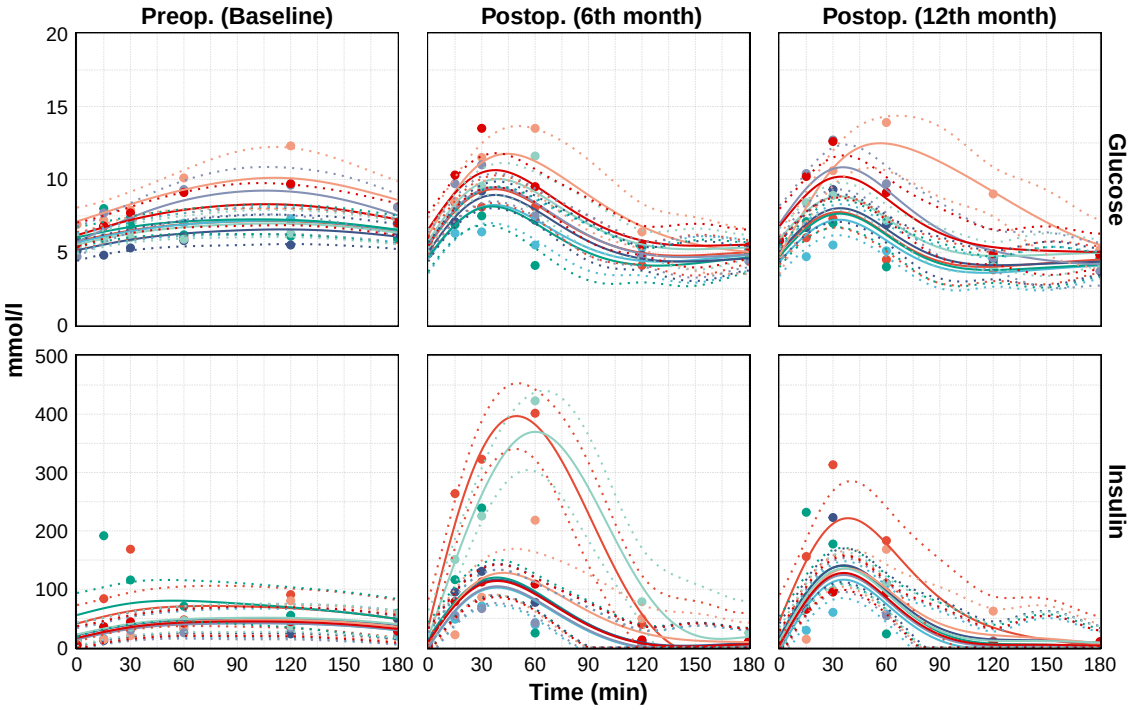

Figure B.2 | Response of the glucose and insulin levels and predicted model fit for different individuals with applied MMT test.

C MMT Model Fitting

MMT includes additional data compared to OGTT. So, for an healthy comparison we trained the model on MMT using the same datapoints exist on the OGTT (partial data). Figure C.1 compares the differences between the model fits with the full data and partial data on MMT.

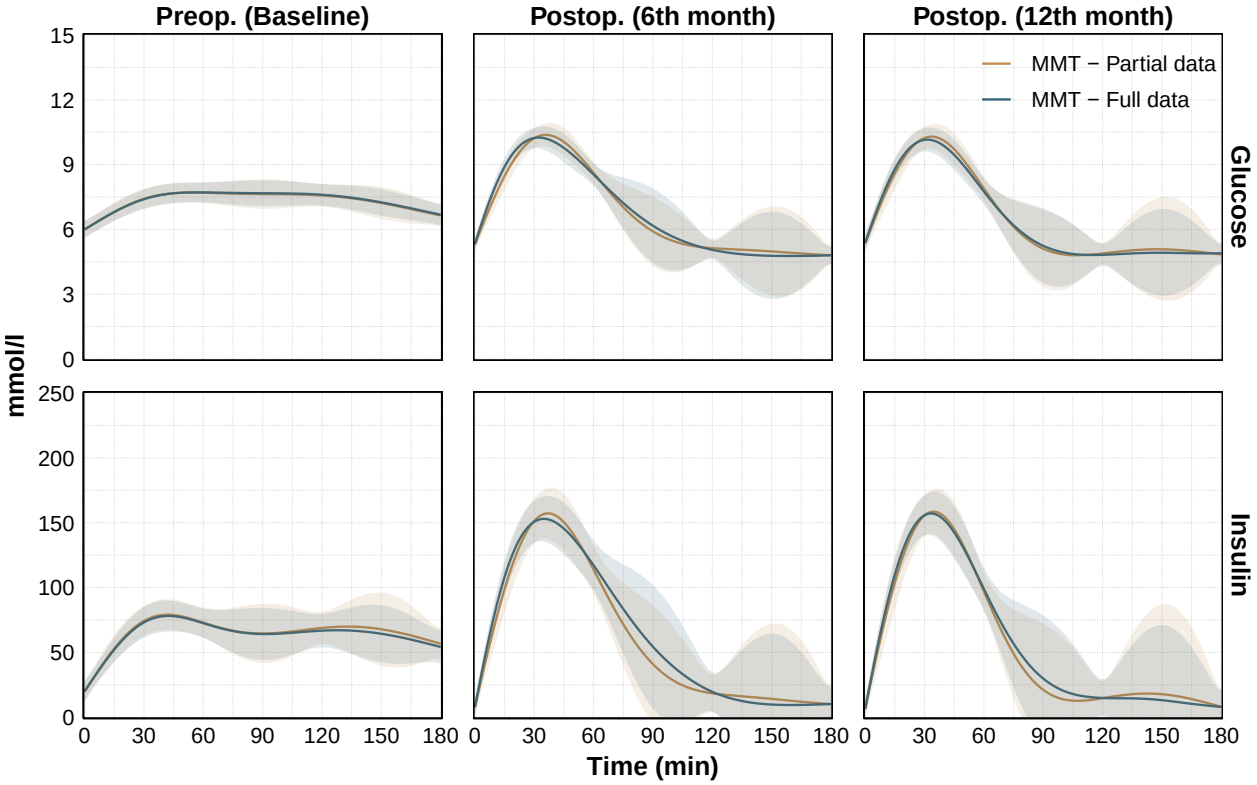

Figure C.1 | Difference of short vs full training results on the MMT.

D Comparison by Diabetes

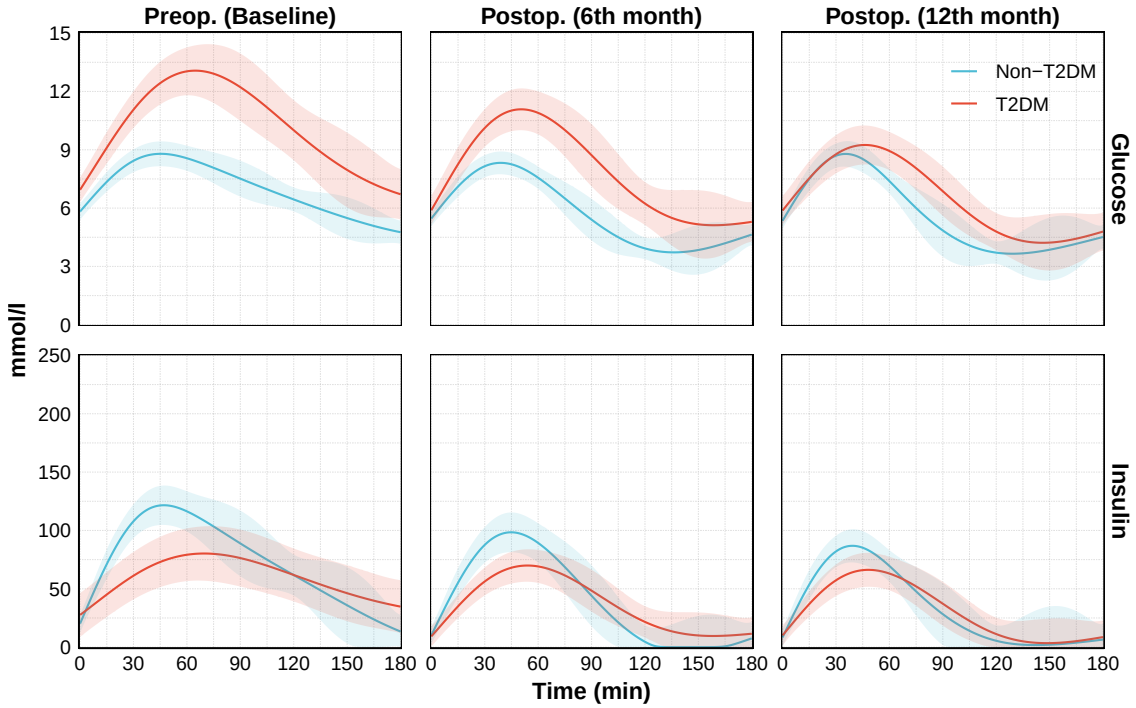

Figure D.1 | The comparison of average glucose and insulin response of the Non-T2DM and T2DM patients in OGTT test.

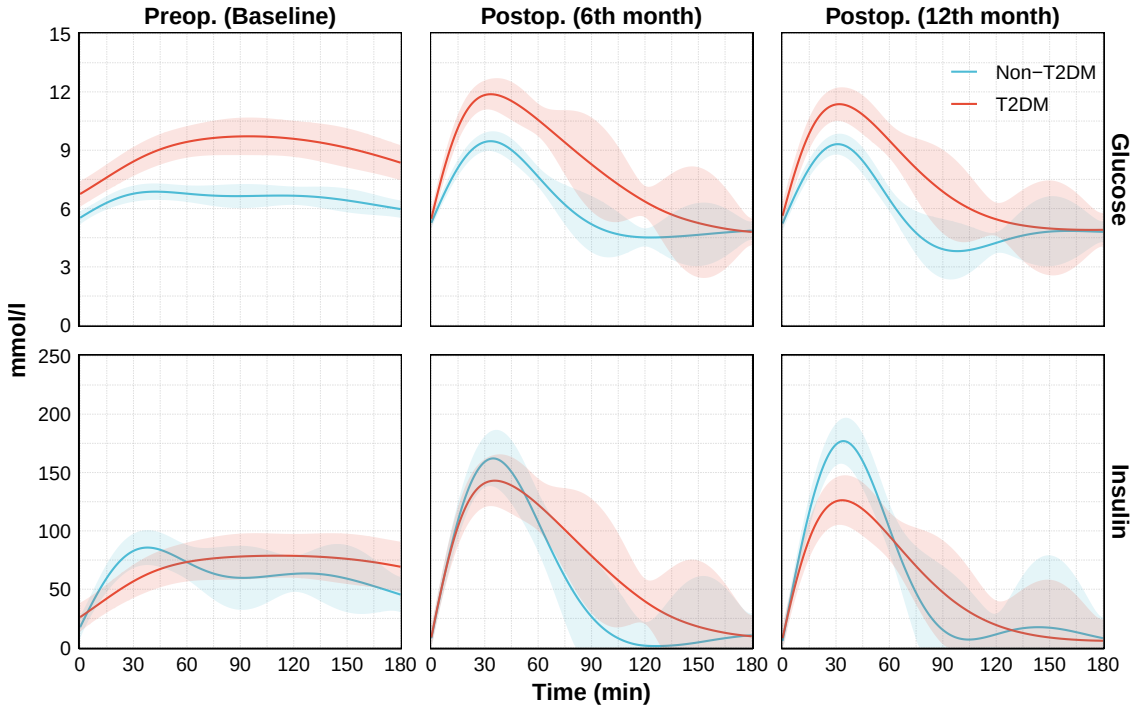

Figure D.2 | The comparison of average glucose and insulin response of the Non-T2DM and T2DM patients in MMT test.

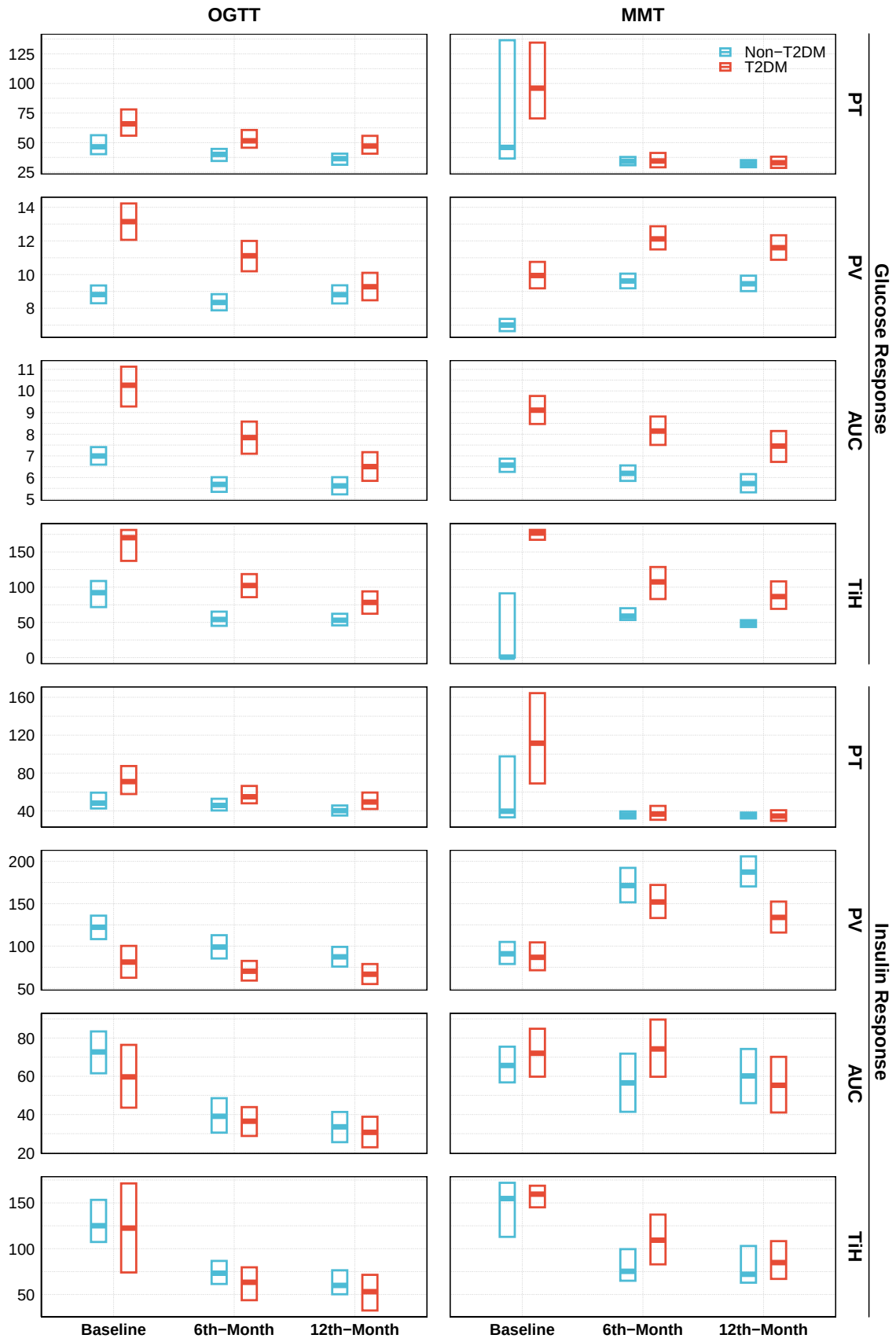

Figure D.3 | Visualization of the metrics for T2DM comparison. See Appendix F for the 95 % CIs and p-values.

E Comparison by Sex

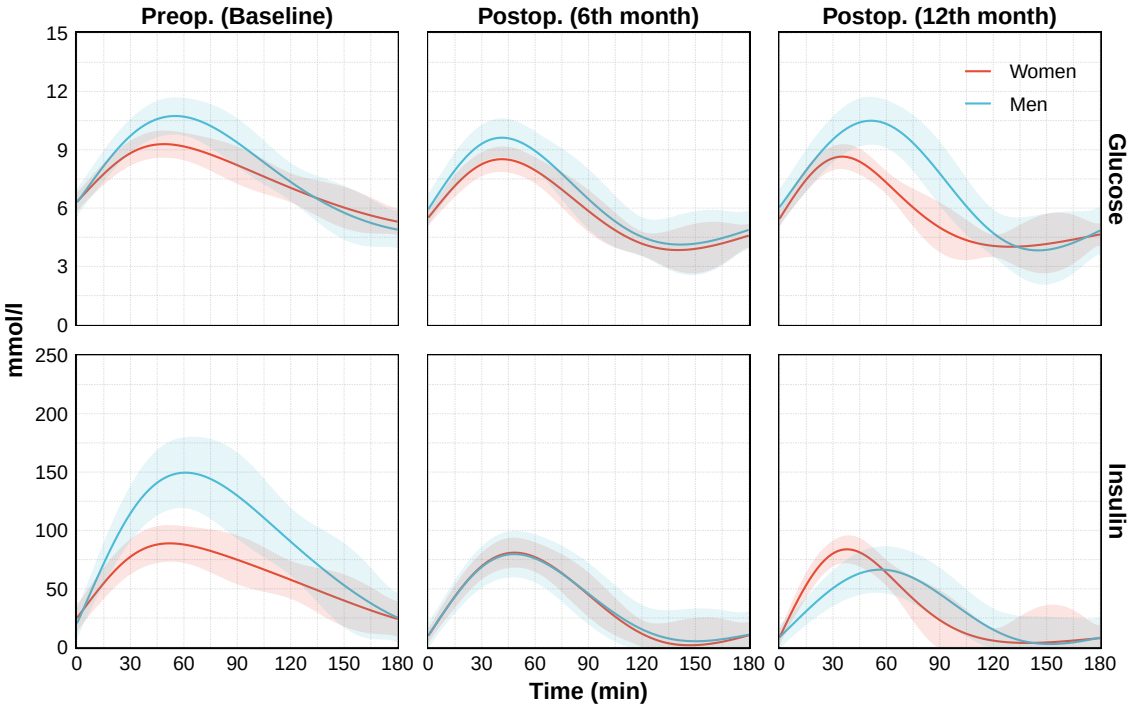

Figure E.1 | The comparison of average glucose and insulin response of the women and men patients in OGTT test.

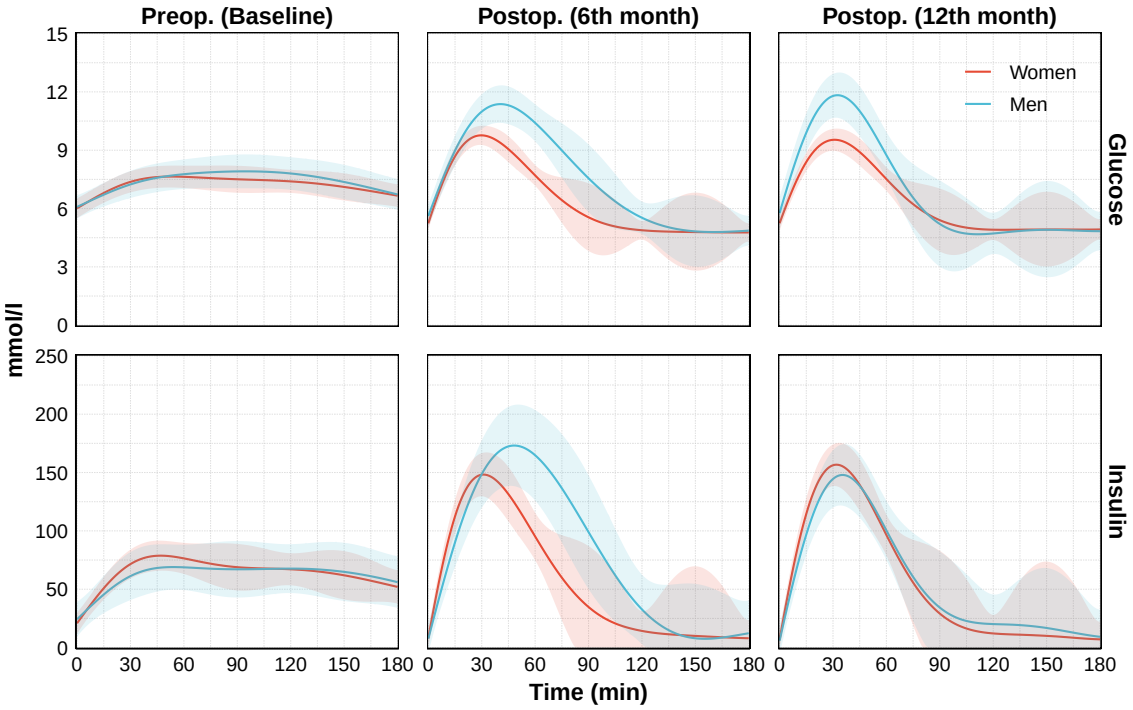

Figure E.2 | The comparison of average glucose and insulin response of the women and men patients in MMT test.

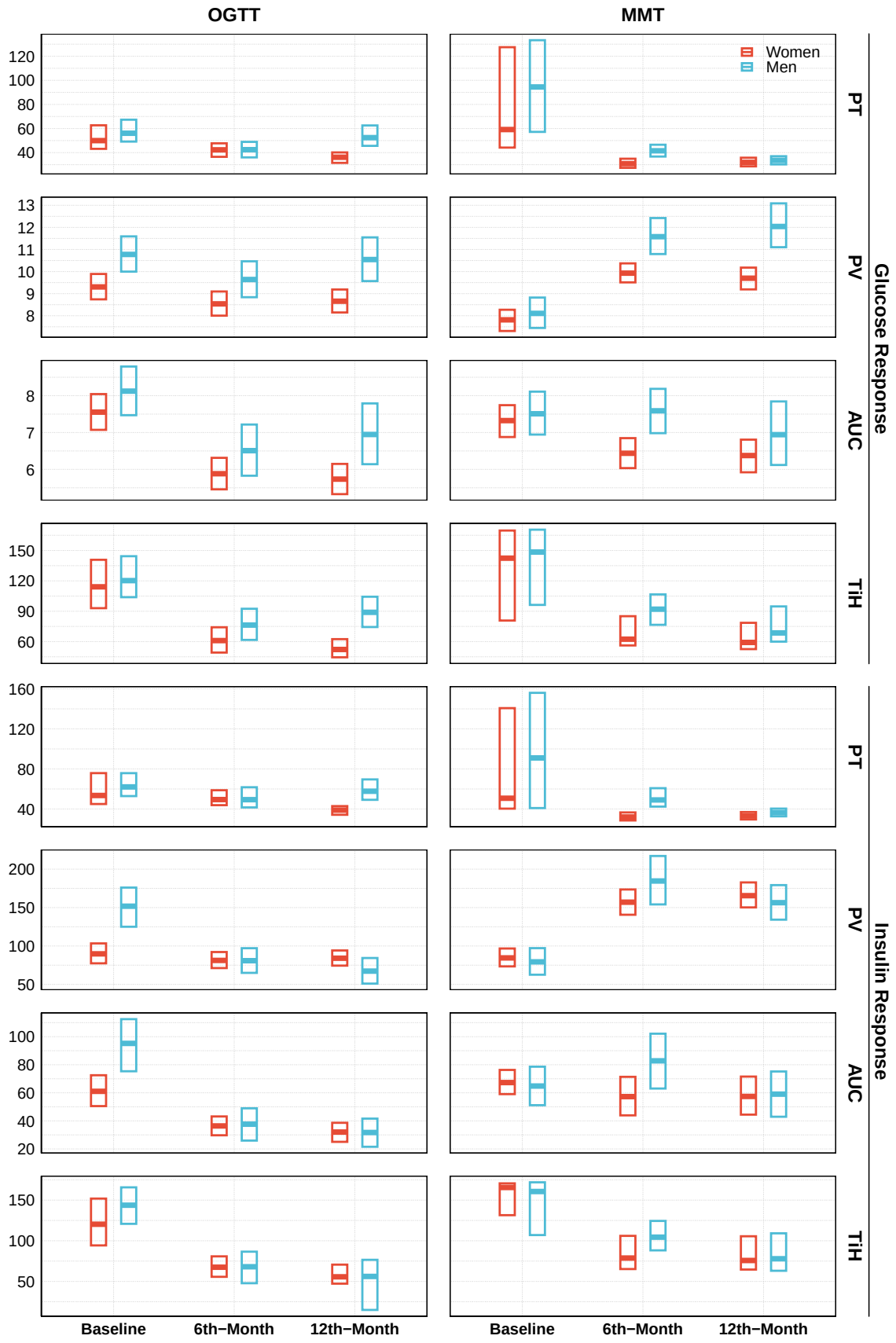

Figure E.3 | Visualization of the metrics for sex comparison. See Appendix F for the 95 % CIs and p-values.

F Evaluation of Metrics

Table F.1 | Peaking time (PT) of the glucose and insulin responses in minutes with 95% confidence intervals and p-values. p-values (except $p(\text{B}\rightarrow12)$) shows the statistical significance of the difference between adjacent cells. $p(\text{B}\rightarrow12)$ represents the statistical significance of the difference between Baseline and 12th month values.

Peaking Time (PT)				**Baseline**	$p(\text{B}\rightarrow6)$	**6th month**	$p(\text{B}\rightarrow12)$	**12th month**
Glucose Response	**Test**	**Overall**	**OGTT**	51 (46-63)	0.011	42 (36-46)	<0.001	39 (34-43)
			p	0.208	-	0.021	-	0.026
			MMT	78 (45-130)	<0.001	33 (29-38)	<0.001	32 (30-36)
	Operation	**OGTT**	**RYGB**	53 (46-70)	0.016	42 (36-47)	<0.001	40 (35-44)
			p	0.392	-	0.373	-	0.469
			OAGB	52 (44-62)	0.097	44 (38-51)	0.022	40 (33-46)
		MMT	**RYGB**	85 (48-134)	<0.001	34 (29-39)	<0.001	32 (29-36)
			p	0.382	-	0.448	-	0.480
			OAGB	71 (46-126)	<0.001	34 (29-38)	<0.001	33 (29-36)
	Diabetes	**OGTT**	**Non-T2DM**	47 (40-56)	0.068	40 (35-45)	0.015	36 (31-41)
			p	0.023	-	0.009	-	0.019
			T2DM	66 (56-78)	0.044	52 (46-61)	0.008	47 (41-56)
		MMT	**Non-T2DM**	46 (37-135)	0.021	34 (31-38)	0.004	32 (29-35)
			p	0.188	-	0.486	-	0.440
			T2DM	96 (70-137)	0.002	34 (29-41)	<0.001	33 (29-38)
	Sex	**OGTT**	**Women**	50 (43-63)	0.065	42 (37-48)	0.002	36 (31-40)
			p	0.266	-	0.469	-	<0.001
			Men	56 (49-67)	0.010	42 (36-49)	0.263	52 (46-63)
		MMT	**Women**	59 (44-127)	<0.001	31 (27-35)	<0.001	32 (29-36)
			p	0.212	-	0.003	-	0.365
			Men	94 (57-133)	0.002	42 (37-47)	<0.001	34 (30-37)
Insulin Response	**Test**	**Overall**	**OGTT**	54 (47-72)	0.238	50 (44-60)	0.014	43 (38-47)
			p	0.291	-	0.002	-	0.015
			MMT	45 (38-146)	0.032	36 (32-41)	0.014	34 (31-38)
	Operation	**OGTT**	**RYGB**	51 (43-70)	0.320	49 (43-57)	0.044	42 (37-47)
			p	0.157	-	0.404	-	0.246
			OAGB	63 (51-79)	0.110	51 (43-63)	0.029	46 (39-55)
		MMT	**RYGB**	45 (36-140)	0.252	41 (34-47)	0.018	33 (30-37)
			p	0.156	-	0.100	-	0.392
			OAGB	84 (47-148)	<0.001	35 (31-39)	<0.001	35 (31-39)
	Diabetes	**OGTT**	**Non-T2DM**	48 (43-59)	0.291	46 (40-53)	0.040	40 (35-46)
			p	0.028	-	0.079	-	0.063
			T2DM	71 (58-87)	0.062	55 (48-66)	0.014	49 (42-59)
		MMT	**Non-T2DM**	40 (33-98)	0.160	36 (32-39)	0.015	35 (32-38)
			p	0.045	-	0.447	-	0.390
			T2DM	112 (69-164)	0.002	37 (31-45)	0.001	35 (30-41)
	Sex	**OGTT**	**Women**	54 (45-76)	0.271	49 (44-59)	0.003	39 (34-43)
			p	0.232	-	0.451	-	0.003
			Men	62 (53-76)	0.070	49 (42-62)	0.290	58 (49-70)
		MMT	**Women**	51 (40-141)	0.002	32 (29-37)	<0.001	33 (30-37)
			p	0.261	-	<0.001	-	0.194
			Men	91 (41-156)	0.151	49 (42-61)	0.012	36 (33-40)

Table F.2 | Peak value (PV) of the glucose and insulin responses in minutes with 95% confidence intervals and p-values. p-values (except $p(\text{B}\rightarrow12)$) shows the statistical significance of the difference between adjacent cells. $p(\text{B}\rightarrow12)$ represents the statistical significance of the difference between Baseline and 12th month values.

Peak Value (PV)				**Baseline**	$p(\text{B}\rightarrow6)$	**6th month**	$p(\text{B}\rightarrow12)$	**12th month**
Glucose Response	**Test**	**Overall**	**OGTT**	9.9 (9.4-10.4)	0.011	9.0 (8.5-9.4)	0.018	9.0 (8.5-9.5)
			p	<0.001	-	<0.001	-	0.004
			MMT	7.8 (7.4-8.2)	<0.001	10.3 (9.9-10.7)	<0.001	10.2 (9.7-10.6)
	Operation	**OGTT**	**RYGB**	10.0 (9.5-10.6)	0.020	9.0 (8.4-9.6)	0.474	10.0 (9.4-10.6)
			p	0.230	-	0.336	-	<0.001
			OAGB	9.6 (8.8-10.4)	0.102	8.8 (8.1-9.4)	0.004	7.8 (7.1-8.5)
		MMT	**RYGB**	7.8 (7.3-8.2)	<0.001	11.4 (10.9-11.9)	<0.001	11.7 (11.2-12.1)
			p	0.388	-	<0.001	-	<0.001
			OAGB	7.6 (7.0-8.2)	0.006	8.8 (8.3-9.3)	0.002	9.1 (8.5-9.7)
	Diabetes	**OGTT**	**Non-T2DM**	8.8 (8.3-9.4)	0.138	8.3 (7.9-8.8)	0.488	8.8 (8.3-9.4)
			p	<0.001	-	<0.001	-	0.214
			T2DM	13.1 (12.1-14.2)	0.010	11.1 (10.2-12.0)	<0.001	9.3 (8.5-10.1)
		MMT	**Non-T2DM**	6.9 (6.6-7.3)	<0.001	9.5 (9.1-9.9)	<0.001	9.3 (8.9-9.8)
			p	<0.001	-	<0.001	-	<0.001
			T2DM	9.8 (9.1-10.6)	<0.001	11.9 (11.3-12.6)	0.008	11.4 (10.7-12.1)
	Sex	**OGTT**	**Women**	9.3 (8.7-9.9)	0.051	8.5 (8.0-9.1)	0.087	8.7 (8.1-9.2)
			p	0.006	-	0.026	-	0.003
			Men	10.8 (10.0-11.6)	0.045	9.6 (8.8-10.5)	0.377	10.5 (9.6-11.5)
		MMT	**Women**	7.7 (7.2-8.2)	<0.001	9.8 (9.4-10.2)	<0.001	9.6 (9.1-10.0)
			p	0.280	-	0.002	-	<0.001
			Men	8.0 (7.4-8.7)	<0.001	11.4 (10.6-12.2)	<0.001	11.8 (10.9-12.8)
Insulin Response	**Test**	**Overall**	**OGTT**	97 (86-109)	0.054	83 (74-93)	0.016	79 (70-89)
			p	0.036	-	<0.001	-	<0.001
			MMT	80 (70-90)	<0.001	154 (139-168)	<0.001	158 (144-172)
	Operation	**OGTT**	**RYGB**	108 (94-123)	0.398	104 (91-119)	0.029	87 (75-100)
			p	0.062	-	<0.001	-	0.062
			OAGB	86 (68-106)	0.091	69 (55-81)	0.124	71 (61-83)
		MMT	**RYGB**	88 (76-101)	<0.001	217 (191-241)	<0.001	187 (169-204)
			p	0.040	-	<0.001	-	<0.001
			OAGB	70 (57-82)	<0.001	122 (106-138)	<0.001	126 (109-142)
	Diabetes	**OGTT**	**Non-T2DM**	122 (108-136)	0.028	99 (85-113)	<0.001	87 (76-99)
			p	0.006	-	0.004	-	0.020
			T2DM	81 (63-100)	0.218	70 (59-83)	0.140	67 (55-79)
		MMT	**Non-T2DM**	87 (75-100)	<0.001	162 (144-182)	<0.001	177 (161-195)
			p	0.360	-	0.120	-	<0.001
			T2DM	83 (68-99)	<0.001	144 (126-163)	0.001	127 (110-145)
	Sex	**OGTT**	**Women**	90 (77-103)	0.203	81 (71-92)	0.288	84 (74-94)
			p	<0.001	-	0.469	-	0.068
			Men	152 (125-176)	<0.001	81 (65-97)	<0.001	67 (51-84)
		MMT	**Women**	81 (70-92)	<0.001	149 (133-164)	<0.001	157 (142-173)
			p	0.340	-	0.087	-	0.281
			Men	76 (60-93)	<0.001	175 (146-205)	<0.001	148 (127-170)

Table F.3 | Area Under Curve (AUC) of the glucose and insulin responses with 95% confidence intervals and p-values. p-values (except $p(\text{B}\rightarrow12)$) shows the statistical significance of the difference between adjacent cells. $p(\text{B}\rightarrow12)$ represents the statistical significance of the difference between Baseline and 12th month values.

Area Under Curve (AUC)				**Baseline**	$p(\text{B}\rightarrow6)$	**6th month**	$p(\text{B}\rightarrow12)$	**12th month**
Glucose Response	**Test**	**Overall**	**OGTT**	7.8 (7.4-8.2)	<0.001	6.1 (5.7-6.4)	<0.001	6.0 (5.6-6.4)
			p	0.098	-	0.026	-	0.117
			MMT	7.4(7.0-7.7)	0.033	6.8 (6.4-7.1)	0.004	6.4 (6.0-6.9)
	Operation	**OGTT**	**RYGB**	8.0 (7.5-8.4)	<0.001	6.1 (5.6-6.5)	<0.001	6.3 (5.8-6.8)
			p	0.129	-	0.460	-	0.094
			OAGB	7.5 (6.8-8.1)	0.004	6.1 (5.6-6.7)	<0.001	5.7 (5.1-6.3)
		MMT	**RYGB**	7.3 (6.8-7.6)	0.381	7.1 (6.7-7.6)	0.120	6.8 (6.3-7.3)
			p	0.494	-	0.012	-	0.156
			OAGB	7.2 (6.7-7.8)	0.013	6.3 (5.8-6.7)	0.034	6.3 (5.8-6.9)
	Diabetes	**OGTT**	**Non-T2DM**	7.0 (6.6-7.4)	<0.001	5.7 (5.3-6.0)	<0.001	5.6 (5.2-6.0)
			p	<0.001	-	<0.001	-	0.025
			T2DM	10.3 (9.3-11.1)	0.002	7.8 (7.1-8.6)	<0.001	6.5 (5.8-7.2)
		MMT	**Non-T2DM**	6.5 (6.2-6.8)	0.090	6.2 (5.8-6.5)	0.005	5.7 (5.3-6.1)
			p	<0.001	-	<0.001	-	<0.001
			T2DM	9.0 (8.4-9.6)	0.049	8.1 (7.4-8.7)	0.004	7.4 (6.7-8.1)
	Sex	**OGTT**	**Women**	7.6 (7.1-8.0)	<0.001	5.9 (5.5-6.3)	<0.001	5.7 (5.3-6.1)
			p	0.116	-	0.092	-	0.016
			Men	8.1 (7.5-8.8)	0.002	6.5 (5.8-7.2)	0.034	6.9 (6.1-7.8)
		MMT	**Women**	7.3 (6.8-7.7)	0.008	6.4 (6.0-6.8)	0.009	6.3 (5.9-6.8)
			p	0.326	-	0.008	-	0.167
			Men	7.4 (6.9-8.0)	0.428	7.5 (6.9-8.1)	0.189	6.9 (6.1-7.8)
Insulin Response	**Test**	**Overall**	**OGTT**	64 (55-73)	<0.001	38 (31-44)	<0.001	33 (27-39)
			p	0.490	-	<0.001	-	<0.001
			MMT	64 (57-72)	0.470	63 (51-75)	0.180	56 (45-68)
	Operation	**OGTT**	**RYGB**	68 (58-79)	0.008	46 (36-55)	<0.001	36 (28-44)
			p	0.200	-	0.040	-	0.203
			OAGB	58 (44-74)	0.006	32 (23-40)	0.002	30 (22-38)
		MMT	**RYGB**	68 (59-79)	0.020	96 (77-112)	0.336	64 (51-79)
			p	0.093	-	<0.001	-	0.048
			OAGB	57 (48-66)	0.162	48 (36-60)	0.104	46 (34-58)
	Diabetes	**OGTT**	**Non-T2DM**	73 (62-83)	<0.001	39 (31-49)	<0.001	34 (26-41)
			p	0.132	-	0.354	-	0.337
			T2DM	60 (44-76)	0.018	37 (29-44)	0.005	31 (23-39)
		MMT	**Non-T2DM**	63 (55-72)	0.197	54 (40-69)	0.289	58 (44-71)
			p	0.261	-	0.079	-	0.353
			T2DM	69 (57-81)	0.408	71 (57-85)	0.078	53 (40-67)
	Sex	**OGTT**	**Women**	61 (51-73)	<0.001	36 (30-43)	<0.001	32 (25-39)
			p	0.009	-	0.446	-	0.494
			Men	95 (75-112)	<0.001	38 (26-49)	<0.001	32 (22-42)
		MMT	**Women**	64 (57-73)	0.141	55 (42-68)	0.151	55 (43-68)
			p	0.400	-	0.042	-	0.454
			Men	62 (49-75)	0.107	79 (60-97)	0.316	57 (41-72)

Table F.4 | Time in the Risk Zone (TiH), where Hyperglycaemia and Hyperinsulinemia are defined as glucose > 7.0mmol/l and insulin > 50mmol/l, respectively, with 95 % confidence intervals and p-values. p-values (except $p(\mathrm{B}\rightarrow 12)$) shows the statistical significance of the difference between adjacent cells. $p(\mathrm{B}\rightarrow 12)$ represents the statistical significance of the difference between Baseline and 12th month values.

Time in the Risk Zone (TiH)				**Baseline**	$p(\mathrm{B}\rightarrow 6)$	**6th month**	$p(\mathrm{B}\rightarrow 12)$	**12th month**
Glucose Response	**Test**	**Overall**	**OGTT**	116 (103-135)	<0.001	66 (56-78)	<0.001	63 (54-75)
			p	0.123	-	0.279	-	0.372
			MMT	144 (109-166)	0.006	72 (63-93)	0.004	61 (55-78)
	Operation	**OGTT**	**RYGB**	125 (110-147)	<0.001	67 (55-80)	<0.001	70 (61-85)
			p	0.085	-	0.484	-	0.036
			OAGB	105 (84-126)	0.006	67 (53-82)	<0.001	47 (20-66)
		MMT	**RYGB**	133 (84-162)	0.052	83 (70-101)	0.032	69 (62-91)
			p	0.464	-	0.014	-	0.054
			OAGB	136 (27-174)	0.090	53 (45-65)	0.091	54 (45-68)
	Diabetes	**OGTT**	**Non-T2DM**	92 (72-109)	0.004	54 (45-65)	<0.001	53 (46-62)
			p	<0.001	-	<0.001	-	0.018
			T2DM	170 (137-181)	0.004	102 (86-119)	<0.001	78 (62-94)
		MMT	**Non-T2DM**	2 (1-74)	0.084	58 (53-68)	0.117	47 (43-52)
			p	<0.001	-	0.001	-	0.001
			T2DM	176 (166-181)	<0.001	106 (82-126)	<0.001	85 (69-107)
	Sex	**OGTT**	**Women**	114 (93-141)	<0.001	61 (49-74)	<0.001	52 (45-62)
			p	0.368	-	0.103	-	0.001
			Men	120 (104-144)	<0.001	76 (62-92)	0.014	89 (74-104)
		MMT	**Women**	136 (65-168)	0.047	61 (55-83)	0.043	58 (52-75)
			p	0.448	-	0.027	-	0.156
			Men	144 (88-169)	0.058	91 (76-106)	0.027	68 (59-93)
Insulin Response	**Test**	**Overall**	**OGTT**	121 (102-148)	<0.001	70 (58-82)	<0.001	59 (50-74)
			p	0.055	-	0.088	-	0.078
			MMT	165 (127-170)	0.004	89 (72-107)	<0.001	74 (64-102)
	Operation	**OGTT**	**RYGB**	125 (107-152)	0.004	80 (68-93)	<0.001	63 (53-79)
			p	0.296	-	0.034	-	0.242
			OAGB	112 (75-154)	0.022	57 (31-74)	0.014	55 (40-71)
		MMT	**RYGB**	168 (124-173)	0.018	108 (90-126)	0.004	80 (68-107)
			p	0.156	-	0.028	-	0.149
			OAGB	148 (83-163)	0.036	67 (57-97)	0.034	64 (55-96)
	Diabetes	**OGTT**	**Non-T2DM**	125 (107-153)	0.002	73 (61-87)	<0.001	60 (50-76)
			p	0.446	-	0.191	-	0.264
			T2DM	122 (74-171)	0.034	63 (44-80)	0.021	53 (33-71)
		MMT	**Non-T2DM**	148 (106-171)	0.009	74 (64-98)	0.009	71 (62-101)
			p	0.385	-	0.054	-	0.296
			T2DM	158 (141-167)	0.016	108 (82-132)	0.003	83 (66-106)
	Sex	**OGTT**	**Women**	120 (94-152)	0.004	67 (56-81)	0.002	56 (47-71)
			p	0.157	-	0.494	-	0.480
			Men	144 (121-166)	<0.001	68 (48-87)	<0.001	56 (15-77)
		MMT	**Women**	163 (125-169)	<0.001	77 (64-105)	0.002	74 (64-104)
			p	0.392	-	0.106	-	0.495
			Men	158 (96-170)	0.074	103 (87-122)	0.032	76 (62-107)

G Data Statistics

Table G.1 | Metabolic features of the patients by different operations and sexes over each visit.

Metabolic Features		Overall	OAGB	RYGB	Male	Female
Age	*Baseline*	46.0 ± 7.0	46.6 ± 7.4	45.4 ± 6.6	50.7 ± 7.4	43.9 ± 5.8
	6th month	46.5 ± 7.0	47.1 ± 7.4	45.9 ± 6.6	51.2 ± 7.4	44.4 ± 5.8
	12th month	47.0 ± 7.0	47.6 ± 7.4	46.4 ± 6.6	51.7 ± 7.4	44.9 ± 5.8
Weight	*Baseline*	130 ± 19	127 ± 15	135 ± 23	138 ± 22	127 ± 17
	6th month	102 ± 16	99 ± 14	107 ± 19	109 ± 18	101 ± 16
	12th month	98 ± 16	94 ± 14	103 ± 18	106 ± 19	95 ± 15
Bmi	*Baseline*	45 ± 6	44 ± 6	46 ± 6	42 ± 5	46 ± 6
	6th month	35 ± 5	35 ± 6	36 ± 5	34 ± 5	37 ± 5
	12th month	34 ± 5	33 ± 6	35 ± 5	33 ± 5	35 ± 5
Hba1c	*Baseline*	39 ± 10	38 ± 6	41 ± 13	38 ± 7	40 ± 11
	6th month	34 ± 5	34 ± 3	33 ± 6	34 ± 4	34 ± 5
	12th month	34 ± 7	34 ± 3	35 ± 10	35 ± 6	34 ± 7
Cholesterol	*Baseline*	4.5 ± 0.9	4.5 ± 1.0	4.6 ± 0.7	4.3 ± 1.3	4.6 ± 0.7
	6th month	3.8 ± 0.7	3.7 ± 0.7	3.9 ± 0.6	3.5 ± 0.8	3.9 ± 0.6
	12th month	3.9 ± 1.0	3.8 ± 0.7	4.3 ± 1.2	3.8 ± 1.1	4.1 ± 0.9
HDL Cholesterol	*Baseline*	1.2 ± 0.2	1.2 ± 0.2	1.2 ± 0.2	1.2 ± 0.2	1.3 ± 0.2
	6th month	1.2 ± 0.2	1.2 ± 0.2	1.3 ± 0.2	1.2 ± 0.2	1.2 ± 0.2
	12th month	1.4 ± 0.3	1.4 ± 0.2	1.4 ± 0.3	1.4 ± 0.3	1.4 ± 0.3
LDL Cholesterol	*Baseline*	2.9 ± 0.8	2.8 ± 0.9	3.0 ± 0.7	2.8 ± 1.1	2.9 ± 0.6
	6th month	2.3 ± 0.7	2.2 ± 0.7	2.4 ± 0.6	2.0 ± 0.7	2.4 ± 0.6
	12th month	2.3 ± 0.8	2.2 ± 0.8	2.3 ± 0.8	2.1 ± 1.1	2.3 ± 0.6
Triglyceride	*Baseline*	1.4 ± 0.7	1.4 ± 0.6	1.4 ± 0.8	1.3 ± 0.6	1.5 ± 0.7
	6th month	1.1 ± 0.4	1.1 ± 0.4	1.1 ± 0.3	0.9 ± 0.3	1.2 ± 0.3
	12th month	1.0 ± 0.3	0.9 ± 0.3	1.0 ± 0.3	0.9 ± 0.3	1.0 ± 0.3
Fasting Glucose	*Baseline*	6.1 ± 1.0	5.9 ± 0.9	6.3 ± 1.2	6.1 ± 0.9	6.1 ± 1.1
	6th month	5.4 ± 0.7	5.4 ± 0.6	5.4 ± 0.8	5.7 ± 0.8	5.3 ± 0.6
	12th month	5.4 ± 0.9	5.4 ± 0.8	5.5 ± 1.0	5.8 ± 1.2	5.3 ± 0.7
Fasting Insulin	*Baseline*	20.3 ± 17.2	20.5 ± 14.7	20.1 ± 20.0	19.1 ± 14.5	20.9 ± 18.5
	6th month	8.2 ± 4.4	8.8 ± 4.6	7.7 ± 4.2	8.4 ± 4.6	8.2 ± 4.4
	12th month	6.6 ± 4.1	7.1 ± 4.6	6.2 ± 3.5	6.7 ± 3.7	6.7 ± 4.3
Fat Kg	*Baseline*	64 ± 13	62 ± 12	65 ± 15	61 ± 16	65 ± 12
	6th month	43 ± 12	41 ± 11	45 ± 12	39 ± 14	45 ± 10
	12th month	38 ± 12	36 ± 13	39 ± 12	31 ± 14	40 ± 11
Fat Percentage	*Baseline*	49 ± 6	49 ± 6	49 ± 7	44 ± 7	51 ± 4
	6th month	41 ± 7	41 ± 8	41 ± 7	35 ± 8	43 ± 5
	12th month	37 ± 9	37 ± 10	38 ± 9	30 ± 9	41 ± 6